those of the controls. In addition, the number and size of the neurons in the posterior horn in the spinal cord appeared to be preserved. These findings indicate that normal development and selective degeneration possibly occurred in the AHCs. It is hardly conceivable that selective developmental retardation occurred in the AHCs, and that developmental retardation of the skeletal muscles induce anterior horn degeneration showing rER reduction. There have been no reports that any congenital muscle dystrophy in mice or humans induces rER reduction in the AHCs.

On the other hand, a decreased number of large neurons and reduced amount of the cytoplasmic RNA, rER and ribosomes, as observed in the spinal cord of *kl/kl* mice, have been noted in the motor neurons in the spinal cord and brain stem of patients with classic ALS [15, 16, 28]; however, Bunina bodies and spheroids were absent in these mice. An accumulation of neurofilaments in the AHCs, as in patients with classic ALS [9, 24, 35], was also reported in the peripheral nerve axon in *kl/kl* mice [41]. Decrease of rER (chromatolysis) and accumulation of neurofilaments have been considered to be early changes in the AHCs in patients with classic ALS [17, 20]. Reactive astrocytosis observed in the anterior horn of the *kl/kl* mice in the present study relates to a degenerative process, and has been reported in the ventral horn in patients with classic ALS. This resemblance shows that *klotho* gene insufficiency causes neuronal dysfunction, and might indicate that the *klotho* gene is involved in the pathological mechanism of classic ALS. Mutant SOD mice may be a good tool for the research of familial ALS [10], and further study is needed to evaluate whether the *kl/kl* mice, which are senescence-accelerated mice showing decreased rER, ribosomes, and cytoplasmic RNA in the AHCs, is a new animal model of AHC degeneration, and can provide clues to understanding the etiology of classic ALS.

Acknowledgements The authors are indebted to Dr. K. Watabe of the Department of Molecular Neuropathology, and Dr. J. Kimura-Kuroda and Dr. I. Nagata (Department of Brain Structure, Tokyo Metropolitan Institute for Neuroscience), Dr. K. Honma (Graduate School of Pharmaceutical Science, University of Tokyo), Ms. M. Shinohara (Department of Anatomy, School of Veterinary Medicine, Tokyo University of Agriculture and Technology), and Dr. A. Mabuchi (Department of Orthopedic Surgery, Graduate School of Medicine, University of Tokyo) for their help during the research. This work was supported in part by grants from the Japanese Ministry of Health, Labor and Welfare (to Y.N., and Research on Psychiatric and Neurological Diseases and Mental Health (H16-kokoro-017 to K.O.)); the Japanese Ministry of Education, Science, Sports and Culture (nos. 12137201 to H.K., 12307031 to K.N., 14657376 to E.K. and 14580735 to K.O.) and the Japan Space Forum (to H.K.).

References

1. Abercrombie M (1946) Estimation of nuclear population from microtome sections. Anat Rec 94:239–247
2. Alberts B, Bray D, Johnson A, Lewis J, Raff M, Roberts K, Walter P (1998) Essential cell biology. Garland, New York
3. Arking DE, Becker DM, Yanek LR, Fallin D, Jdge DP, Moy TF, Becker LC, Dietz HC (2003) KLOTHO allele status and the risk of early-onset occult coronary artery disease. Am J Hum Genet 72:1154–1161
4. Babu KA, Verma RS (1985) Structural and functional aspects of nucleolar organizer regions (NORs) of human chromosomes. Int Rev Cytol 94:151–171
5. Bailey AA (1953) Changes with age in the spinal cord. Arch Neurol Psychiatry 70:299–309
6. Baldini A, Marleka P (1985) Hormone-modulated rRNA gene activity is visualized by selective staining of the NOs. Cell Biol Int Rep 9:791–796
7. Brustmann H, Riss P, Naude S (1995) Nucleolar organizer regions as markers of endometrial proliferation: a study of normal, hyperplastic, and neoplastic tissue. Hum Pathol 26:664–667
8. Buys CHCM, Osinga J, Anders GJPA (1979) Age-dependent variability of ribosomal RNA-gene activity in man as determined from frequencies of silver staining nucleolus organizing regions of metaphase chromosomes of lymphocytes and fibroblasts. Mech Ageing Dev 11:55–75
9. Carpenter S (1968) Proximal axonal enlargement in motor neuron disease. Neurology 18:841–851
10. Cleveland DW, Rothstein JD (2001) From Charcot to Lou Gehrig: deciphering selective motor neuron death in ALS. Nat Rev Neurosci 2:806–8199
11. Crocker J, Boldy DAR, Egan MJ (1989) How should we count AgNORs? Proposals for a standardized approach. J Pathol 158:185–188
12. Fushiki S, Kinoshita C, Tsutsumi Y, Nishizawa Y (1995) Age-related changes of the argyrophilic nucleolar organizer regions in mouse neocortical neurons. Acta Histochem Cytochem 28:533–538
13. Gaubatz J, Cutler RG (1978) Age-related differences in the number of ribosomal RNA genes of mouse tissue. Gerontology 24:179–207
14. Goodpasture C, Bloom SE (1975) Visualization of nucleolar organizer regions in mammalian chromosomes using silver staining. Chromosoma 53:37–50
15. Hartmann HA, McMahon S, Sun DY, Abbs JH, Uemura E (1989) Neural RNA in nucleus ambiguous and nucleus hypoglossus of patients with amyotrophic lateral sclerosis. J Neuropathol Exp Neurol 48:669–673
16. Hirano A (1991) Cytopathology of amyotrophic lateral sclerosis. Adv Neurol 56:91–101
17. Hirano A, Inoue K (1980) Early pathological changes of amyotrophic lateral sclerosis. Electron microscopic study of chromatolysis, spheroids and Bunina bodies. Neurol Med 13:148–160
18. Howell WM, Black DA (1980) Controlled silver staining of nucleolus organizer regions with a protective colloidal developer: a 1-step method. Experientia 36:1014–1015
19. Hubbell HR (1985) Silver staining as an indicator of active ribosomal genes. Stain Technol 60:285–294
20. Inoue K, Hirano A (1979) Early pathological changes of amyotrophic lateral sclerosis. Autopsy findings of a case of 10 months' duration. Neurol Med 11:448–455
21. Jimenez R, Burgos M, Diaz de la Guardia R (1988) A study of the Ag-staining significance in mitotic NORs. Heredity 60:125–127
22. Johnson R, Stehler BL (1972) Loss of genes coding for ribosomal RNA in ageing brain cells. Nature 240:412–414
23. Johnson RW, Chrisp C, Stehler BL (1972) Selective loss of ribosomal RNA genes during the ageing of post-mitotic tissues. Mech Ageing Dev 1:183–198
24. Julien JP (1995) A role for neurofilaments in the pathogenesis of amyotrophic lateral sclerosis. Biochem Cell Biol 73:593–597
25. Kameyama T, Hashizume Y, Sobue G (1996) Morphologic features of the normal human cadaveric spinal cord. Spine 21:1285–1290

26. Kawamura Y, O'Brien P, Okazaki H Dyck PJ (1977) Lumbar motoneurons of man. II. The number and diameter distribution of large-and intermediate-diameter cytons in "motoneuron columns" of spinal cord of man. J Neuropathol Exp Neurol 36:861–870
27. Kuro-o M, Matsumura Y, Aizawa H, Kawaguch H, Suga T, Utsugi T, Ohyama Y, Kurabayashi M, Kaname T, Kume E, Iwasaki H, Iida A, Shiraki-Iida T, Nishikawa S, Nagai R, Nabeshima Y (1997) Mutation of the klotho gene leads to a syndrome resembling ageing. Nature 390:45–51
28. Mann DMA, Yates PO (1974) Motor neuron disease: the nature of the pathogenic mechanism. J Neuropathol Exp Neurol 37:1036–1046
29. Matsumura Y, Aizawa H, Shiraki-Iida T, Nagai R, Kuro-o M, Nabeshima Y (1998) Identication of the human klotho gene and its two transcripts encoding membrane and secreted Klotho protein. Biochem Biophys Res Commun 242:626–630
30. Morton CC, Brown JA, Holmes WM, Nance WE, Wolf B (1983) Stain intensity of human nucleolus organizer region reflects incorporation of uridine into mature ribosomal RNA. Exp Cell Res 145:405–413
31. Nielsen AL, Nyholm HC, Engel P (1994) Expression of MIB-1 (Paraffin ki-67) and AgNOR morphology in endometrial adenocartinomas of endometrioid type. Int J Gynecol Pathol 13:37–44
32. Niwa K, Yokoyama Y, Tanaka T, Mori H, Mori H, Tamaya T (1991) Silver-stained nucleolar organizer regions in the normal, hyperplastic and neoplastic endometrium. Virchows Arch [A] 29:493–497
33. Rexed B (1952) The cytoarchitectonic organization of the spinal cord in the cat. J Comp Neurol 96:415–495
34. Ruschoff J, Plate K, Bittinger A, Thomas C (1989) Nucleolar organizer regions (NORs). Basic concepts and practical application on tumor pathology. Pathol Res Pract 185:878–885
35. Schmidt M L, Carden MJ, Lee VM, Trojanowski JQ (1987) Phosphate dependent and independent neurofilament epitopes in the axonal swellings of patients with motor neuron disease and controls. Lab Invest 56:282–294
36. Schulte EK, Lyon HO, Hoyer PE (1992) Simultaneous quantitafication of DNA and RNA in tissue sections. A comparative analysis of the methyl green-pyronin technique with the gallocyanin chromalum and Feulgen procedures using image cytometry. Histochem J 24:305–310
37. Terao S, Sobue G, Hashizume Y, Li M, Inagaki T, Mitsuma T (1996) Age-related changes in human spinal ventral horn cells with special reference to the loss of small nerurons in the intermediate zone: a quantitative analysis. Acta Neuropathol 92:109–114
38. Thomas S, Mukherjee AB (1996) A longitudinal study of human age-related ribosomal RNA gene activity as detected by silver-stained NORs. Mech Ageing Dev 92:101–109
39. Tohyama O, Imura A, Iwao A, Freund JN, Henrissat B, Fujimori T, Nabeshima Y (2004) Klotho is a novel beta-glucuronidase capable of hydrolyzing steroid beta-glucuronides. J Biol Chem 279:9777–9784
40. Tomlinson BE, Irving D (1977) The number of limb motor neurons in the human lumbosacral cord throughout life. J Neurol Sci 34:213–219
41. Uchida A, Komiya Y, Tashiro T, Yorifuji H, Kishimoto T, Nabeshima Y, Hisanaga S (2001) Neurofilaments of Klotho, the mutant mouse prematurely displaying symptoms resembling human aging. J Neurosci Res 64:364–370
42. Vargas JP, Rodríguez F, Lépez JC, Arias JL, Salas C (2000) Spatial learning-induced increase in the argyrophilic nucleolar organizer regions of dorsolateral telencephalic neurons in goldfish. Brain Res 865:77–84
43. Wilkinson N, Buckley H, Chawner L, Fox H (1990) Nucleolar organizer regions in normal, hyperplastic, and neoplastic endometria. Int J Gynecol Patho l 9:55–59

Journal of Neuroscience Research 75:678–687 (2004)

Distinctive Expression of Midkine in the Repair Period of Rat Brain During Neurogenesis: Immunohistochemical and Immunoelectron Microscopic Observations

Kae Kikuchi-Horie,[1,2] Emiko Kawakami,[1] Makiko Kamata,[3] Manabu Wada,[1,4] Jian-Guo Hu,[3] Hachiro Nakagawa,[3] Kazuhiko Ohara,[1,2] Kazuhiko Watabe,[5] and Kiyomitsu Oyanagi[1]*

[1]Department of Neuropathology, Tokyo Metropolitan Institute for Neuroscience, Tokyo, Japan
[2]Department of Veterinary Anatomy, Faculty of Agriculture, Tokyo University of Agriculture and Technology, Tokyo, Japan
[3]Research and Development Center, BML, Saitama, Japan
[4]The Third Department of Internal Medicine, Yamagata University School of Medicine, Yamagata, Japan
[5]Molecular Neuropathology, Tokyo Metropolitan Institute for Neuroscience, Tokyo, Japan

Distinctive expression of midkine (MK) was observed during the repair period of fetal brain neuroepithelium. MK is a heparin-binding growth factor that occurs as a product of a retinoic acid-inducible gene, and has a molecular mass of 13 kDa. MK expression was examined immunohistochemically and by immunoelectron microscopy during a period of repair in developing rat brain at the neurogenesis stage. Injury was induced in rat fetuses by transplacental administration of ethylnitrosourea (ENU) on embryonic Day (E) 16, and histological changes were examined up to 48 hr thereafter (i.e., up to E 18). In normal rat fetuses, MK immunostaining was observed in the cytoplasm and radial and horizontal processes of all cells in the neuroepithelium (NE), subventricular zone (SV), and intermediate zone (IMZ). In ENU-administered brains, cells in the NE, SV, and IMZ were damaged severely, especially 16–24 hr after ENU administration. The remaining neuroepithelial cells, with the exception of those in M-phase and the tips of processes at the ventricular surface, were negative for MK immunohistochemistry 16–24 hr after the administration of ENU. Forty-eight hours after the administration, the cytoplasm and processes of cells in the NE, SV, and IMZ were MK immunopositive. Our previous data reported that the cell cycle of most NE cells is synchronized to the S-phase 16 hr after ENU administration and to the M-phase at 24 hr, and many NE cells were recovered 48 hr after ENU administration. The previous results taken together with the present results indicate that: (1) MK expression does not increase during the repair period of the NE, being different from adults; (2) MK expression is likely to be suppressed at S-phase according to the condition of the NE; and (3) MK expression is not essential for every cell cycle phase of NE cells; but (4) is necessary to maintain the M-phase of NE cells.

Key words: cell cycle; ethylnitrosourea; lesion repair; midkine; neuroepithelium

Midkine (MK) is a heparin-binding growth factor that occurs as a product of a retinoic acid-inducible gene, and has a molecular mass of 13 kDa (Muramatsu, 1994). MK has been reported as involved in neurogenesis and neuron differentiation, in neurite outgrowth (Michikawa et al., 1993; Muramatsu et al., 1993; Matsuzawa et al., 1999), and neuronal survival (Michikawa et al., 1993; Satoh et al., 1993; Matsuzawa et al., 1999). In the developing brain, MK has been reported to occur in the neuroepithelium (NE) (Muramatsu et al., 1993; Mitsiadis et al., 1995), migrating neurons, and processes of radial glia (Matsumoto et al., 1994; Sun et al., 1997, 1999). The MK receptor-like protein tyrosine phosphatase PTPζ/RPTPβ has been observed in migrating neurons and processes of radial glia of the fetal rat brain, suggesting the involvement of MK in neuroblast migration (Maeda and Noda, 1998; Maeda et al., 1999). MK has also been detected in various organs during the mid-gestation period of embryogenesis and is considered to be involved in regulation of organogenesis (Kadomatsu et al., 1990; Mitsiadis et al., 1995). MK expression decreases gradually with age, and in normal adult mice is expressed persistently only in the kidney

Jian-Guo Hu is currently at Fuji Photo Optical Co., Saitama, Japan.

*Correspondence to: Kiyomitsu Oyanagi, MD, PhD, Department of Neuropathology, Tokyo Metropolitan Institute for Neuroscience, 2-6 Musashidai, Fuchu, Tokyo 183-8526, Japan. E-mail: k123ysm@tmin.ac.jp

Received 28 July 2003; Revised 6 November 2003; Accepted 19 November 2003

Published online 2 February 2004 in Wiley InterScience (www.interscience.wiley.com). DOI: 10.1002/jnr.20015

(Kadomatsu et al., 1990; Nakamoto et al., 1992; Muramatsu et al., 1993).

During the repair period in adults, it has been reported that MK expression is upregulated in adults with gastric ulcer (Maekawa et al., 1999) and bone fracture (Ohta et al., 1999), and that MK is expressed in reactive astrocytes in the ischemic rat brain (Satoh et al., 1993; Mochizuki et al., 1998; Wang et al., 1998). MK was reported to be produced around the site of nerve damage in early stages of experimental cerebral infarction in adult rats (Yoshida et al., 1995). We reported recently that MK immunoreactivity was observed in astrocytes especially in the early period of ischemic brain lesions in human adults (Wada et al., 2002).

Regarding the repair mechanism in developing brain, during the repair process of the irradiation-injured developing fetal brain, a reduction in number and irregularity of shape of MK-immunopositive processes of radial glia has been reported (Sun et al., 1997). The abnormal cytoarchitecture of the cortical neurons was considered to be induced by abnormal migration of neuroblasts along with the irregularly arranged MK-immunopositive processes of radial glia (Sun et al., 1999). The following points, however, remain to be established: (1) whether MK expression in the fetal brain changes during the repair period at the stage of neurogenesis; and (2) whether MK expression in NE cells changes in relation to the kinetics during the repair period. These clarifications are considered essential for elucidation of the biological significance of MK in the developing brain.

We examined immunohistologically and by immunoelectron microscopy the time course of alterations of MK expression in fetal rat brains at the neurogenesis stage after injury by transplacental administration of ethylnitrosourea (ENU). One main effect of ENU is to block DNA synthesis (Swann and Magee, 1971), resulting in microcephalus or cortical and spinal cord dysgenesis in rats (Hallas and Das, 1978, 1979; Fujiwara, 1980; Houle and Das, 1984; Yoshida et al., 1984; Oyanagi et al., 1986, 1987, 1988, 1998, 2001) up to 48 hr after the administration, when repair of the injured NE is completed (Fujiwara, 1980; Yoshida et al., 1984; Oyanagi et al., 1986, 1987, 1988). A single intravenous injection of ENU (60 mg/kg body weight) does not disrupt the glial limitans over the cerebrum or tight junctions of NE cells, and does not induce hemorrhage, tissue laceration, or heterotopic mass (Yoshida et al., 1984; Oyanagi et al., 1986, 2001). The transplacental administration of ENU thus enables us to analyze precisely the repair mechanism in the cellular unit of fetal brain after injury, because it preserves the essential framework of the brain except for damage to proliferating cells.

MATERIALS AND METHODS

The experimental procedure used to induce lesions was essentially the same as that reported previously (Oyanagi et al., 1986, 1998). The research project was approved by the Ethics Committee of the Tokyo Metropolitan Institute for Neuroscience (TMIN) and conformed to provisions of the Declaration of Helsinki in 1995. Adequate measures were taken to minimize pain and discomfort to the animals according to the Guidelines for Animal Experiments of the TMIN.

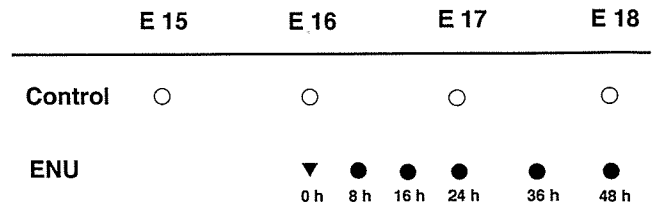

Fig. 1. Experimental protocol. Down triangle, ENU, 60 mg/kg body weight, intravenous administration to the dams; open/filled circles, sacrifice; E, embryonic day; h, hours after ENU administration.

Animals

For experiments, 2–4-month-old albino Wistar rats (weighing 250–300 g) were used. Virgin females were mated with males for one night, and vaginal smears were examined on the next morning. The day on which sperm was observed was designated as embryonic Day 1 (E 1). All rats were housed individually and provided with food and water ad lib in an air-conditioned room under a 12:12-hr light:dark cycle.

Terminology

The terminology used to describe the developing cerebral neocortex has been revised several times during the past three decades. In the present work, the embryonic neocortex is divided into six basic zones that lie parallel to the ventricular surface. The neuroepithelium (NE) (Bayer and Altman, 1991) is a proliferating ventricular zone lining the ventricles that consists of a compact layer of columnar bipolar cells. The subventricular zone (SV) (Boulder Committee, 1970; Bayer and Altman, 1991) is composed of small cells that are round or oval. The intermediate zone (IMZ) (Boulder Committee, 1970; Bayer and Altman, 1991) is a layer with a relatively low number of cells composed of horizontally or irregularly arranged bipolar or star-shaped cells. The subplate (SP) (Bayer and Altman, 1991) is a zone with a relatively low number of cells with sparse cell processes. The cortical plate (CP) (Boulder Committee, 1970; Bayer and Altman, 1991) is a mass of neuroblasts in the process of differentiating into neurons. The marginal zone (MZ) (Boulder Committee, 1970) is a zone of cell processes and a few small round cells.

Induction of NE Injury

The degree of tissue injury to the NE at the neurogenesis stage is proportional to the dose of ENU administered (Fujiwara, 1980; Yoshida et al., 1984). In the present study, a single intravenous injection of ENU (60 mg/kg body weight) was administered to maintain the glia on the brain surface and the tight junctions of the NE cells of the neocortex (Yoshida et al., 1984; Oyanagi et al., 1986, 1987, 1998, 2001). On E 16, each of the 40 pregnant rats was given a single tail vein injection of ENU that had been freshly dissolved in physiological saline. The time at the completion of the injection was designated as 0 hr (Fig. 1).

Sampling of Brain Tissues

Fetuses were removed by cesarean section from ether-anesthetized dams at 8, 16, 24, 36, and 48 hr after ENU administration. For MK Western blotting, brains were removed and cerebri were frozen. For immunohistochemical examination, fetuses were sacrificed by perfusion of the heart with 0.1 M phosphate buffer (PB; pH 7.3) containing 1% heparin followed by 4% paraformaldehyde in 0.1 M PB. The embryonic brain tissue was removed and immersed in the same fixative in 0.1 M PB for 24 hr. For MK immunohistochemistry, tissue blocks were then transferred into 30% sucrose in 0.1 M PB. Blocks of tissues were embedded in Tissue-Tek OCT compound (Miles Inc.) at −80°C and cut in the frontal plane (20 μm thickness) by cryostat (Leitz 1720; Leica, Germany). Observation was carried out in the dorsal neocortex at the E 16 Coronal 6 level of Paxinos et al. (1994). Fetuses sacrificed on E 15, 16, 17, and 18 served as controls. Eight fetuses from different dams (four each for MK and SMI immunohistochemistry) were investigated in each group of ENU-administered and normal rats for the immunohistological and Western blotting.

Primary Antibody Against MK

The primary antibody against MK used was the same as that used recently for the study of ischemic human brain lesions (Wada et al., 2002). Briefly, the MK antibody used for immunostaining and immunoblotting was generated in rabbit. Purified recombinant human MK (0.5 mg) was emulsified in a mixture of Freund's complete adjuvant (1:1) and 0.25 mg/ml of heparin. The emulsion was injected subcutaneously into the animal's back. They were boosted on alternate weeks in the same manner, except that 0.25 mg MK and incomplete Freund's adjuvant were used. Antisera collected 1 week after the fourth and fifth inoculations were purified by affinity chromatography of the MK peptide (Peptide Institute, Osaka, Japan) coupled with cyanogen bromide (CNBr)-activated Sepharose 4B (Pharmacia Biotech, Uppsala, Sweden).

MK Western Blotting

Immunoblotting was carried out using the right occipital lobe without evident pathologic alteration of a 68-year-old female patient who died of bronchopneumonia and mitral stenosis, and using the cerebri of the normal and ENU-administered rats. The cerebral tissue was cut into pieces and sonicated in 0.1 g/ml homogenization buffer (10 mM Tris, pH 7.4, 1% Triton X-100, 1 M NaCl, and 0.5 mM phenylmethylsulfonyl fluoride). After centrifugation at 20,000 × *g* for 1 hr, the resulting supernatant was incubated with heparin Sepharose for 16 hr at 4°C before being loaded. After thorough washing with 0.5 N NaCl and 0.1 M phosphate-buffered saline (PBS), heparin-binding proteins, including MK, were eluted with 1.5 N NaCl plus PBS.

The eluate was concentrated by ultrafiltration through a MW 3,000 membrane. Samples containing 1.33 mg cerebral tissue were subjected to SDS-PAGE using a 5–20% gradient gel, and were then transferred onto an Immobilon-P membrane (Millipore, Bedford, MA). The membrane was first incubated with the anti-MK antibody (2 μg/ml diluted in PBS containing 1% skimmed milk) for 16 hr at 4°C, followed by treatment with anti-rabbit IgG conjugated with horseradish peroxidase (1:5,000; Zymed, San Francisco, CA). Immunopositive signals were detected with the aid of a chemiluminescence reagent (NEN/DuPont, Boston, MA; Fig. 2). Based on densitometric data obtained from the bands, quantification of the amount of MK per 1.3 mg of the brain tissue of the fetuses was attempted (Fig. 2C,D). All MK and pleiotrophin (PTN) used as standards in Western blotting in this study were purchased from the Peptide Institute (Osaka, Japan). Statistical evaluation was carried out using the Mann-Whitney U-test.

MK Immunohistochemistry

For immunohistochemical examinations, sections dried for one night at 37°C were immersed in diethyl ether for 10 min at room temperature (RT). The avidin-biotin-peroxidase complex (ABC) method (Vectastain; Vector, Burlingame, CA) was used. After removal of the OCT compound, intrinsic peroxidase activity in the tissue was blocked by incubation with 1% hydrogen peroxide for 20 min. Sections were first blocked with 10% normal goat serum in 0.01 M PBS and subsequently incubated with anti-MK antibody (10 μg/ml) in 0.01 M PBS containing 0.03% Triton X-100 (PBST) at 4°C for 48 hr. Sections were then incubated with the secondary reagent containing biotinylated anti-rabbit IgG (diluted 1:200) in 0.01 M PBST for 2 hr and finally with the avidin-biotin complex for 1 hr at RT. Peroxidase labeling was visualized by incubating the sections with 0.05 M Tris-HCl buffer, pH 7.6, containing 0.05% 3,3′ diaminobenzidine tetrahydrochloride (DAB), 0.05 M imidazole, and 0.0008% hydrogen peroxide for 10 min at RT to yield a brown reaction product. Sections were counterstained lightly with 0.5% methyl green. As antibody controls, the primary antiserum was either omitted or replaced with normal rabbit serum. Several specimens of neural and nonneural tissue from rats served as positive or negative tissue controls. Sections from four fetuses from different dams were used to rule out individual variability in development or in the effectiveness of ENU. Four fetuses, one each at E 15, 16, 17, and 18, from different dams served as controls.

MK Immunoelectron Microscopic Observations

Electron microscopic observations were carried out on samples from E 17 normal brains and from brains of E 17 fetuses 24 hr after ENU administration. MK-immunostained frozen sections were recycled. After post-fixation with 1% osmium tetroxide in 0.1 M PB, sections were dehydrated in a graded ethanol series up to absolute ethanol. A capsule containing Epon 812 resin was placed on each section and then polymerized at 60°C. After the Epon block had been removed from the glass slide, ultrathin sections were cut and stained with lead citrate. Observations were carried out using an H-9000 electron microscope (Hitachi, Tokyo, Japan). We defined "normal looking cells" as cells showing a normal appearance without apoptotic features such as apoptotic bodies or nuclear condensation.

RESULTS

MK Western Blotting

In the Western blot analysis, one distinct band at 16 kDa was observed in heparin-binding protein from adult human normal brain tissue (Fig. 2A, lane 2 and 3),

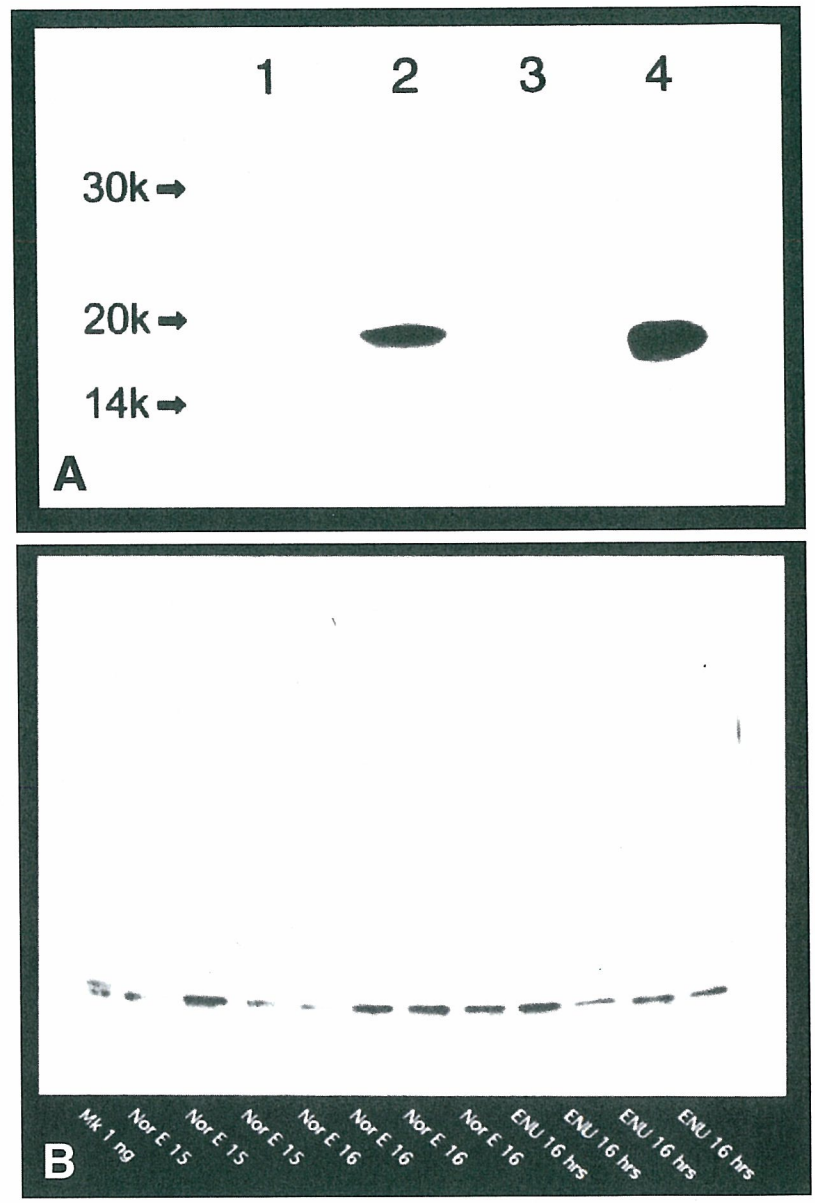

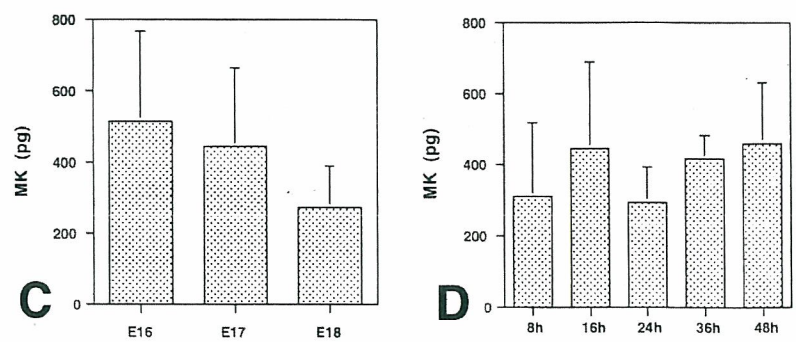

Fig. 2. Midkine (MK)-Western blotting. **A:** MK in the brain extract from a 68-year-old female. The rabbit anti-MK antibody did not show cross-reactivity with human pleiotrophin (PTN), even though 100 ng was used. **Lane 1,** human PTN 100 ng; **lane 2, 3,** heparin Sepharose-purified human brain extract 42 μg, and 14 μg, respectively; **lane 4,** human MK 20 ng. The molecular marker is shown on the left. **B:** Recombinant human MK, 1 ng, and 1.33 mg cerebral tissue of each group were examined. **C, D:** Quantification of MK per 1.33 mg brain tissue. Graphs show mean + SD. C, normal; D, ENU-treated. Nor, normal; E, embryonic day; ENU, ethylnitrosourea administered; h, hours after ENU administration.

and recombinant human MK (Fig. 2A, lane 4). The anti-MK antibody did not cross react with human pleiotrophin/heparin-binding growth-associated molecule (PTN/HB-GAM; Fig. 2A, lane 1), even though 100 ng was used. Use of the pass-through fraction preabsorbed with human MK markedly reduced MK immunoreactivity (data not shown). One distinct band was also observed in heparin-binding protein from each

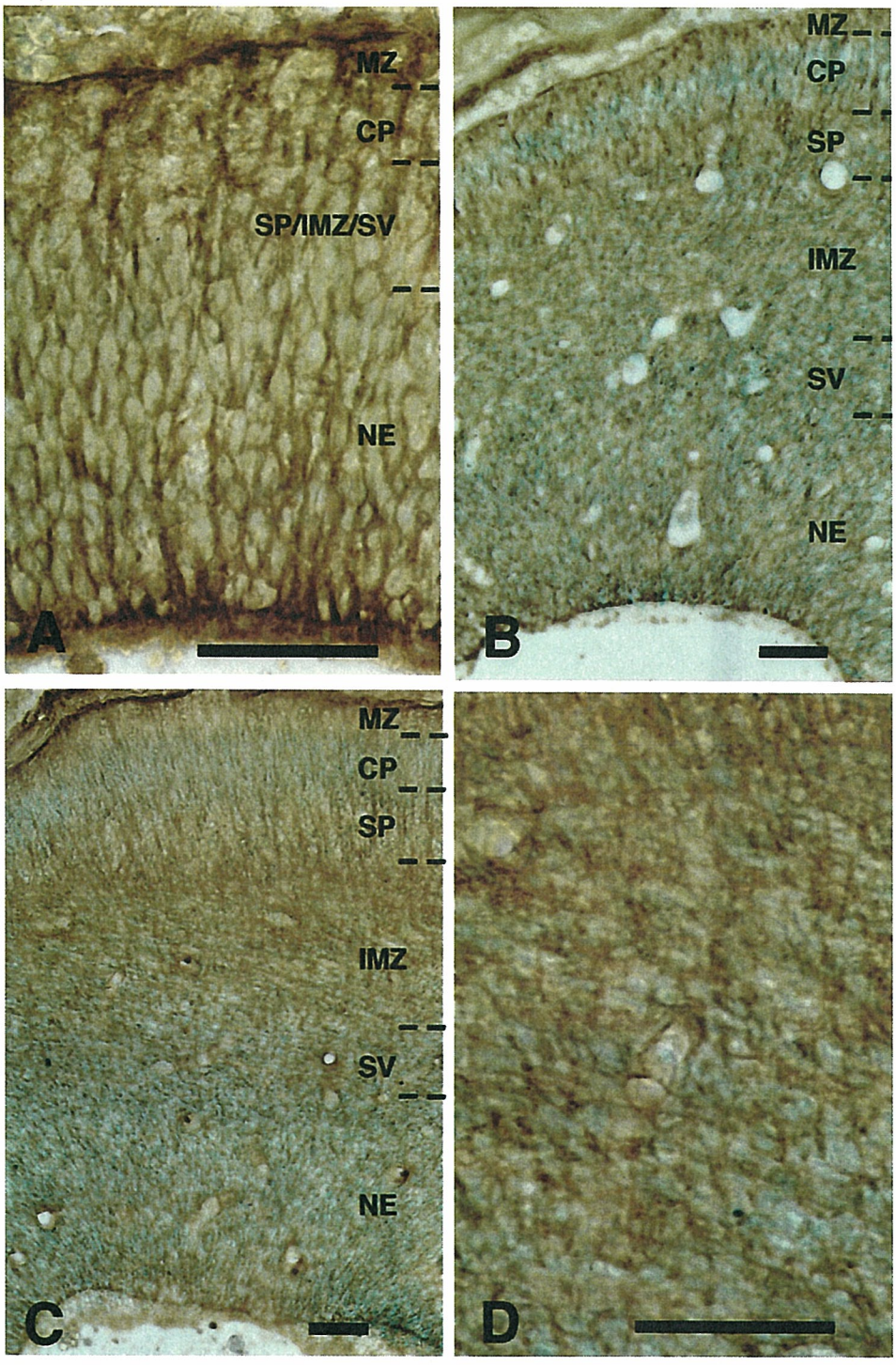

Fig. 3. Immunohistochemistry for MK in the dorsal cerebral neocortex of control animals E 16–18. Counterstained with methyl green. (**A**) Normal E 16; (**B**) normal E 17; (**C**) normal E 18; (**D**) intermediate zone (IMZ) of normal E 18. NE, neuroepithelium; SV, subventricular zone; IMZ, intermediate zone; SP, subplate; CP, cortical plate; MZ, marginal zone. Scale bars = 50 μm.

brain tissue of normal and ENU-administered rats (Fig. 2B). Although the data obtained were not significant statistically, the amount of MK in the normal fetal brain showed a tendency to decrease with development from E 16 to E 18 (Fig. 2C). An increase in MK was not evident in brains of ENU-treated rat fetuses (Fig. 2D).

MK Immunohistochemistry

Strong MK immunoreactivity in the normal fetal brain was observed in cytoplasm and processes of all cells in the NE, SV, and IMZ on E 15 and 16 (Fig. 3A). MK immunoreactivity was relatively strong in cell processes, perpendicular and horizontal to the ventricle wall, in the

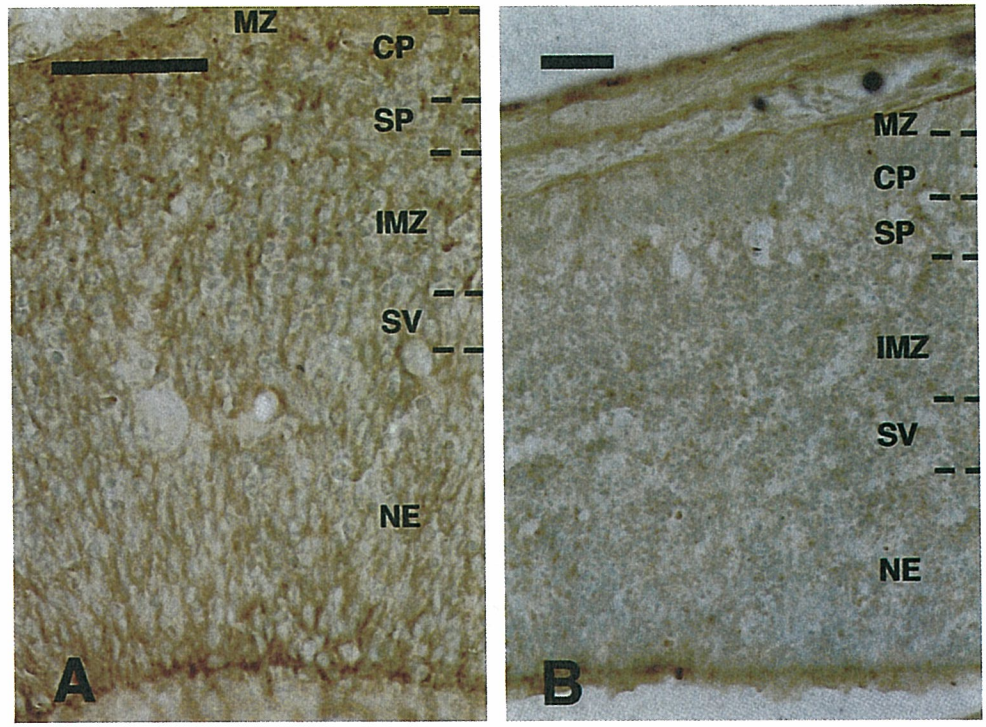

Fig. 4. Immunohistochemistry for MK in the dorsal cerebral neocortex 8 (**A**) and 16 hr (**B**) after ENU injection. Counterstained with methyl green. In ENU-treated rat fetuses 8 hr after administration, MK-immunoreactivity in cytoplasm and processes of the cells in the NE, SV, and IMZ was weaker than that of normal E 16 tissue. Sixteen hours after ENU administration, immunoreactivity in cytoplasm and processes in the NE, SV, and IMZ was weak, but fine granular immunoreactivity appeared in the IMZ and NE. NE, neuroepithelium; SV, subventricular zone; IMZ, intermediate zone; SP, subplate; CP, cortical plate; MZ, marginal zone. Scale bars = 50 μm.

IMZ on E 17 and 18 (Fig. 3B–D). MK immunopositivity was not seen in the nuclei (Fig. 3A–D) or the cytoplasm of cells in the CP (Fig. 3B,C).

In the ENU-treated rat fetuses 8 hr after administration, MK immunoreactivity in the cytoplasm and processes of the cells in the NE, SV, and IMZ was weaker than that of normal E 16 tissue (Fig. 4A). Sixteen hours after ENU administration, immunoreactivity in cytoplasm and processes in the NE, SV, and IMZ was weak, but fine granular immunoreactivity appeared in the IMZ and NE (Fig. 4B). Twenty-four hours after ENU administration, the amount of fine granular MK immunoreactivity had increased further, and MK-immunopositive cytoplasm and processes of the cells in the NE, SV, and IMZ were observed only rarely (Fig. 5A). MK immunoreactivity was abolished completely by omitting the anti-MK antibody (Fig. 5B). Immunoelectron microscopic observation of MK revealed strong immunoreactivity in the cytoplasm and cell processes of NE cells and migrating neuroblasts in the IMZ of normal E 17 fetal brain. All cell processes in the NE and IMZ were positive for MK immunostaining (data not shown). Conversely, no immunostaining was seen in the cytoplasm and processes of migrating neuroblasts, NE cells, and radial glia 24 hr after ENU administration. Only the cytoplasm of NE cells in the M-phase and processes along the ventricular surface were densely immunopositive for MK 24 hr after ENU administration (Fig. 5C). Fine granular MK immunostaining was localized exclusively within apoptotic cells, but not observed in normal-looking cells in the NE, SV, and IMZ (Fig. 5D).

The amount of fine granular immunoreactivity of MK had decreased 36 hr after ENU administration, and MK immunoreactivity in the IMZ, corresponding to migrating neuroblasts and NE cells and processes were stronger than that observed at 16 and 24 hr. Clustering of MK-immunopositive material in the IMZ (Fig. 6A,B) considered to be phagocytes containing apoptotic cells observed previously (Oyanagi et al., 1986). Fine granular immunoreactivity was greatly decreased 48 hr after ENU administration, and cytoplasm and processes of all cells in the NE, SV, and IMZ were immunopositive for MK (Fig. 6B). NE cells along with ventricular surface, which are considered to be in M-phase, were positive for MK-immunohistochemistry at each period during the observation (Fig. 3–6). Neither the nuclei nor the cytoplasm of cortical plate cells were immunopositive for MK (Fig. 3–5).

DISCUSSION

ENU is known to be a neurogenic resorptive carcinogen (Druckrey et al., 1972; Bosch, 1977a), and to have a cytotoxic effect immediately after administration (Bosch et al., 1972). ENU has been reported to impair cellular DNA synthesis by alkylating the bases, and to decompose in intact animals with a half-life of less than 20 min (Swann and Magee, 1971). ENU has been found to induce selective degeneration of proliferating cells (Bosch, 1977b) or cells in the S- to M-phase of the cell cycle in developing brain (Yoshida et al., 1984), and temporary cell-cycle arrest in or before the S-phase (Bosch and Ebels, 1976). Transplacental ENU administration to fetuses has been reported to result in microcephalus, paucity of dendrites, and a reduction in neuronal cytoplasm in the central nervous system (Hallas and Das, 1978, 1979),

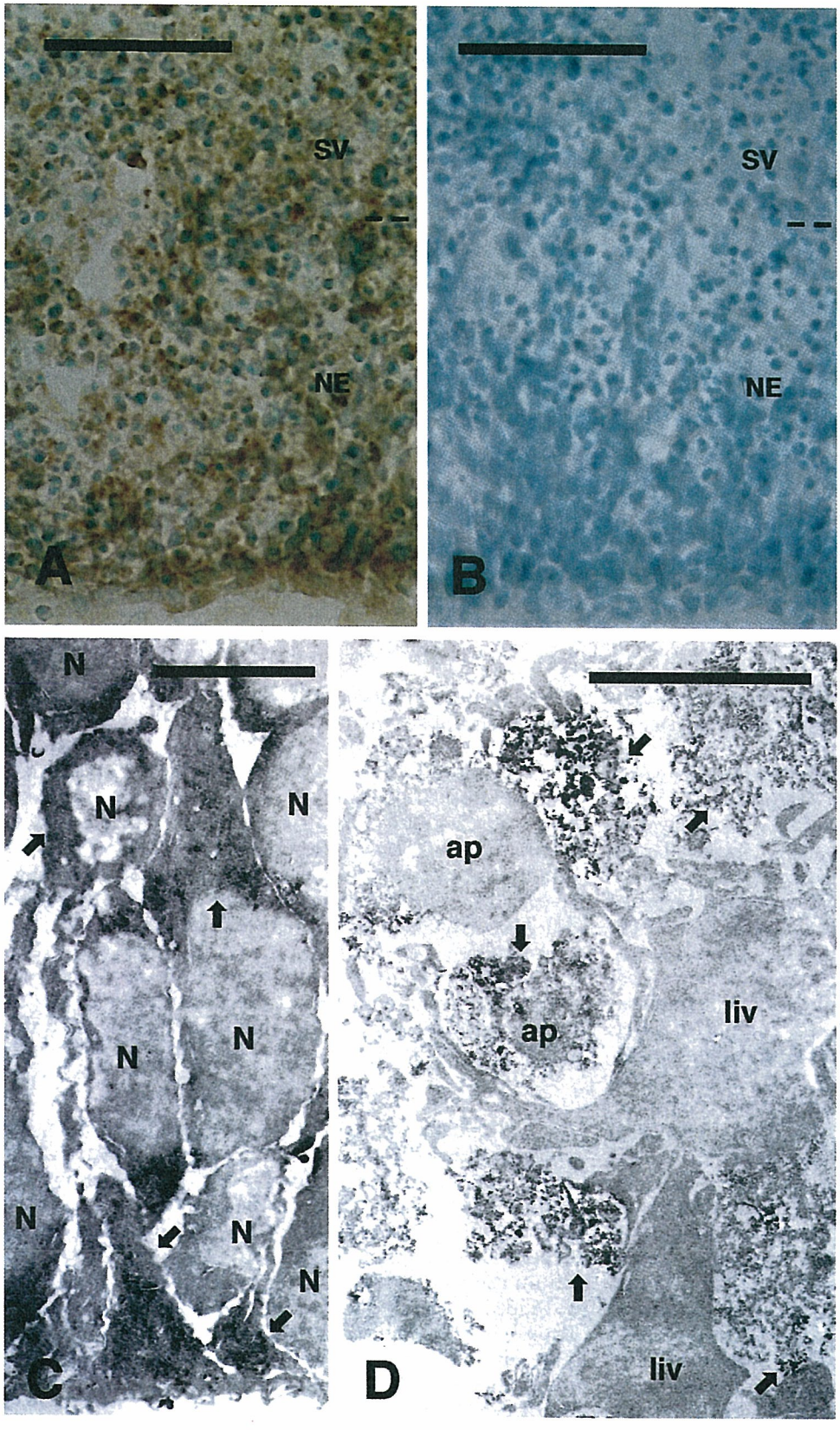

Fig. 5. Immunohistochemistry for MK in the neuroepithelium (NE) and subventricular zone (SV) at the dorsal cerebral neocortex 24 hr after ENU injection. **A:** NE; amount of fine granular MK immunoreactivity had increased further and MK-immunopositive cytoplasm and cell processes in the NE, SV, and IMZ were observed only rarely. **B:** MK immunoreactivity is abolished completely by omitting anti-MK antibody. Scale bars = 50 μm. Immunoelectron microscopic findings of MK-immunohistochemistry. **C:** Ventricular surface of NE 24 hr after ENU administration. **D:** NE 24 hr, only the cytoplasm of NE cells in the M-phase and processes along ventricular surface were densely immunopositive for MK. Fine granular MK-immunostaining was localized exclusively within the apoptotic cells, but not observed in normal looking cells in the NE, SV, and IMZ. Arrowheads, MK immunoreactivity; N, nucleus; liv, normal-looking cell; ap, apoptotic cell. Scale bars = 5 μm.

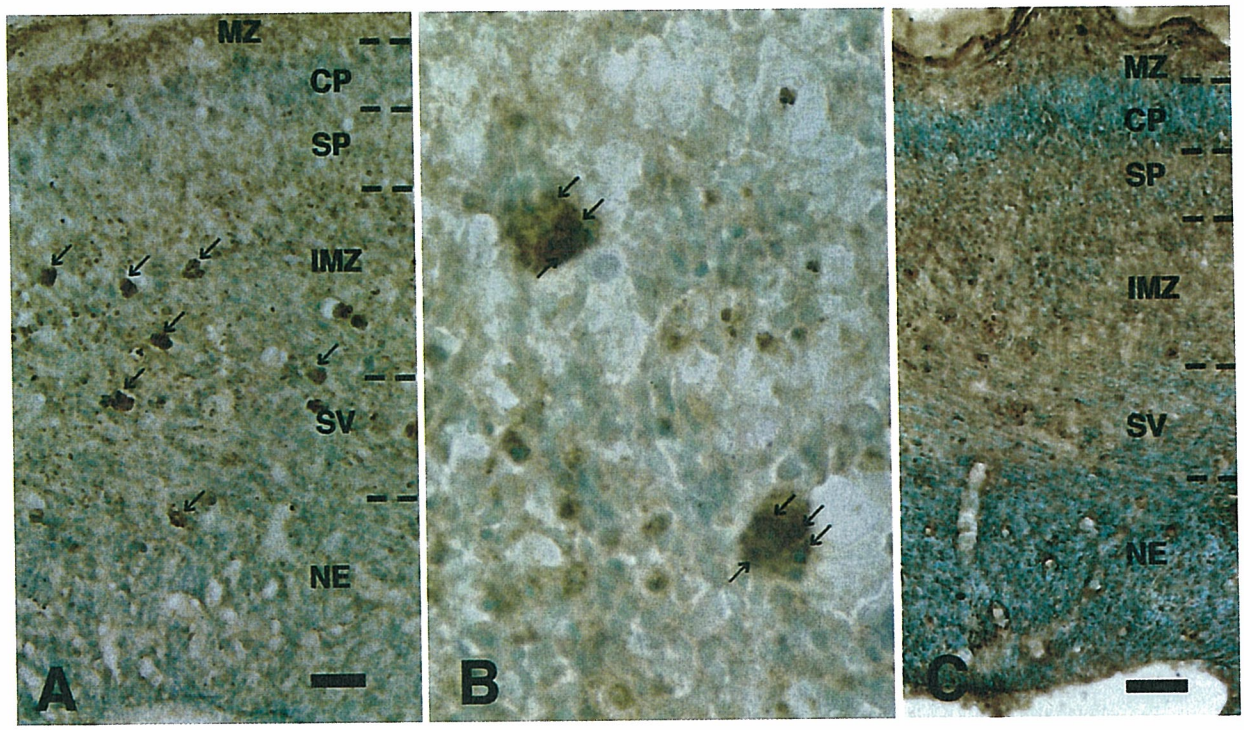

Fig. 6. Immunohistochemistry for MK in dorsal cerebral neocortex 36 and 48 hr after ENU injection. **A:** Arrows indicate clustering of MK-immunopositive material. **B:** High-power view of A. Arrows show nuclei of MK-immunopositive cells. Counterstained with methyl green. A and B, 36 hr; **C**, 48 hr. NE, neuroepithelium; SV, subventricular zone; IMZ, intermediate zone; SP, subplate; CP, cortical plate; MZ, marginal zone. Scale bars = 50 μm.

and the severity of fatal brain tissue damage is controllable by the amount of ENU (Fujiwara, 1980; Yoshida et al., 1984).

During neurogenesis, the NE of spinal cord and the external granular cell layer of cerebellum are able to regenerate within a certain period after injury (Altman et al., 1969; Shimada and Langman, 1970; Houle and Das, 1984; Ferrer et al., 1995). It has been reported previously that ENU administration (60 mg/kg body weight) to the developing rat brain at the neurogenesis stage results in: (1) severe damage to NE cells, migrating neuroblasts, and processes of radial glia, especially 16–24 hr after administration; (2) temporary arrest of NE cell cycle in the G1-phase 4–8 hr after administration; (3) cell cycle synchronization of most NE cells to the S-phase at 16 hr after administration and to the M-phase 24 hr thereafter; and (4) recovery of many cells in the NE 48 hr after administration of ENU (Oyanagi et al., 1998).

In the present study, MK was expressed continuously in the cytoplasm of the NE cells, radial and perpendicular processes, and in the postmitotic migrating neuroblasts, but disappeared in the cytoplasm of immature neurons after arriving at the cortical plate in the normal developing brain. During the repair period of the developing brain, however, fine granular MK immunostaining was localized exclusively within apoptotic cells but not observed in normal-looking cells in the NE, SV, and IMZ 24 hr after ENU administration. This indicates that MK expression was suppressed in the living NE cells, when most NE cells are in the S- to G2-phase (Oyanagi et al., 1998). NE cells in the M-phase and the tips of cell processes at the ventricular surface, however, were always positive for MK immunohistochemistry. This shows that MK is necessary for the M-phase of NE cells and that MK might be essential for keeping junctional complex of NE cells (Fig. 7). Continuous MK expression in NE cells at the M-phase may relate to the potential function of MK to induce cell proliferation (Ratovitski et al., 1998; Kato et al., 1999; Qiu et al., 2000).

In the normal fetal brain at the neurogenesis stage, all processes of cells in NE and IMZ were immunopositive for MK; thus, "radial glia", if they would exist, are positive for MK immunohistochemistry. It was observed in the present study that after ENU administration, alteration of MK expression in cells and processes in the NE was quite synchronized. This finding suggests that ENU promotes synchronization of the kinetics of NE cells and radial glia, if any, or that the processes of radial glia are the processes of the NE cells (Fujita, 1963; Fujita and Fushiki, 1983; Ikuta et al., 1984) (Fig. 7).

MK has been reported to be a secreted protein (Muramatsu and Muramatsu, 1991). In the present study and as reported previously, however, MK immunostaining was observed exclusively inside cells. This finding may be

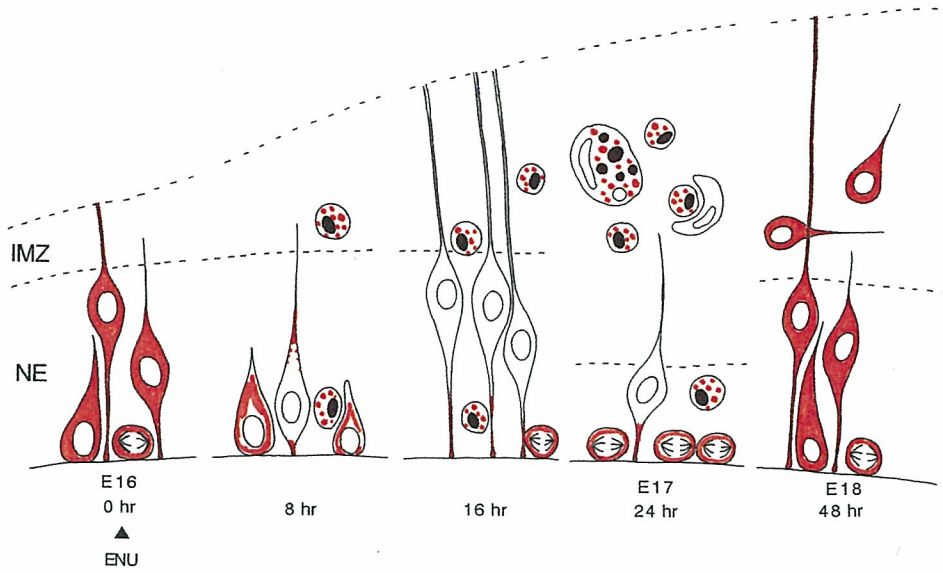

Fig. 7. Schematic demonstration of MK expression (orange) in early stage of repair process of developing rat brain at neurogenesis. Bipolar or unipolar cells are NE cells or migrating neuroblasts; round cells showing mitosis along ventricular wall are NE cells in M-phase, and round cells containing MK-immunopositive granules are apoptotic cells. IMZ, intermediate zone; NE, neuroepithelium.

the result of internalization of secreted MK into the cytoplasm (Ohta et al., 1999), and washing out of the MK from the extracellular spaces during rinsing of sections in the immunohistochemistry protocol.

The findings of the neuroepithelial cells observed in the present study indicate that: (1) MK expression does not increase during the repair period of the neuroepithelium, being different from adults; (2) MK expression is likely to suppressed at the S-phase according to the condition of the neuroepithelium; and (3) MK expression is not essential for every phase of the cell cycle of neuroepithelial cells; but (4) is necessary to maintain the M-phase of the neuroepithelial cells (Fig. 7).

ACKNOWLEDGMENTS

We thank Ms. Y. Kawazoe of the Department of Molecular Neuropathology and Ms. A. Nakamura of the Department of Neuropathology (Tokyo Metropolitan Institute for Neuroscience) for technical advice. We also thank Dr. H. Kawano and Dr. M. Horie of the Department of Anatomy and Development (Tokyo Metropolitan Institute for Neuroscience) for their help, and Dr. H. Shibata and Professor N. Kanda of the Faculty of Agriculture, Tokyo University of Agriculture and Technology for allowing us the opportunity to carry out this research.

REFERENCES

Altman J, Anderson WJ, Write KA. 1969. Reconstitution of the external granular cell layer of the cerebellar cortex in infant rats after low-level X-irradiation. Anat Rec 163:453–472.

Bayer SA, Altman J. 1991. Neocortical development. New York: Raven Press.

Bosch DA. 1977a. Short and long term effects of methyl- and ethylnitrosourea (MNU and ENU) on the developing nervous system of the rat. I. Long term effects: the induction of (multiple) gliomas. Acta Neurol Scand 55:85–105.

Bosch DA. 1977b. Short and long term effects of methyl- and ethylnitrosourea (MNU and ENU) on the developing nervous system of the rat. II. Short term effects: concluding remarks on chemical neuro-oncogenesis. Acta Neurol Scand 55:106–122.

Bosch DA, Ebels EJ. 1976. Temporary cell cycle arrest in neural and extraneural developing rat tissues after exposure to methyl and ethylnitrosourea. Z Krebsforsch Klin Onkol Cancer Res Clin Oncol 86:23–31.

Bosch DA, Gerrits PO, Ebels EJ. 1972. The cytotoxic effect of ethylnitrosourea and methylnitrosourea on the nervous system of the rat at different stages of development. Z Krebsforsch Klin Onkol Cancer Res Clin Oncol 77:308–318.

Boulder Committee. 1970. Embryonic vertebrate central nervous system: revised terminology. Anat Rec 166:257–262.

Druckrey H, Ivankovic S, Preussmann R, Zülch KJ, Mennel HD. 1972. Selective induction of malignant tumors of the nervous system by resorptive carcinogen. In: Kirsch WM, Grossi-Paoletti E, Paoletti P, editors. The experimental biology of brain tumors. Springfield, IL: Charles C Thomas. p 85–147.

Ferrer I, Barrón S, Rodríquez-Farré E, Planas AM. 1995. Ionizing radiation-induced apoptosis is associated with c-Jun expression and c-Jun/AP-1 activation in the developing cerebellum of the rat. Neurosci Lett 202:105–108.

Fujita S. 1963. The matrix cell and cytogenesis in the developing central nervous system. J Comp Neurol 120:37–42.

Fujita S, Fushiki S. 1983. [Significance of cell movement in the histogenesis of the nervous system]. Tanpakushitsu Kakusan Koso 28:469–487.

Fujiwara H. 1980. Cytotoxic effects of ethylnitrosourea on central nervous system of rat embryos. Special references to carcinogenesis and teratogenesis. Acta Pathol Jpn 30:375–387.

Hallas BH, Das GD. 1978. *N*-ethyl-*N*-nitrosourea-induced teratogenesis of brain in the rat. J Neurol Sci 39:111–122.

Hallas BH, Das GD. 1979. An aberrant nucleus in the telencephalon following administration of ENU during neuroembryogenesis. Teratology 19:159–164.

Houle JD, Das GD. 1984. Tissue repair in the embryonic rat spinal cord following exposure to *N*-ethyl-*N*-nitrosourea. Int J Dev Neurosci 2:1–11.

Ikuta F, Yoshida Y, Ohama E, Oyanagi K, Takeda S, Yamazaki K, Watabe K. 1984. Brain and peripheral nerve edema as an initial stage of the lesion repair: revival of the mechanisms of the normal development in the fetal brain. Shinkei Kenkyu No Shimpo 28:599–628.

Kadomatsu K, Huang RP, Suganuma T, Murata F, Muramatsu T. 1990. A retinoic acid responsive gene MK found in the teratocarcinoma system is expressed in spatially and temporally controlled manner during mouse embryogenesis. J Cell Biol 110:607–616.

Kato S, Ishihara K, Shinozawa T, Yamaguchi H, Asano Y, Saito M, Kato M, Terada T, Awaya A, Hirano A, Dickson DW, Yen SH, Ohama E. 1999. Monoclonal antibody to human midkine reveals increased midkine expression in human brain tumors. J Neuropathol Exp Neurol 58:430–441.

Maeda N, Ichihara-Tanaka K, Kimura T, Kadomatsu K, Muramatsu T, Noda M. 1999. A receptor-like protein-tyrosine phosphatase PTPζ/RPTPβ binds a heparin-binding growth factor midkine. J Biol Chem 274:12474–12479.

Maeda N, Noda M. 1998. Involvement of receptor-like protein tyrosine phosphataseζ/RPTPβand its ligand pleiotrophin/heparin-binding growth-associated molecule (HB-GAM) in neuronal migration. J Cell Biol 142:203–216.

Maekawa T, Waki S, Okada A, Fukui H, Kinoshita Y, Chiba T. 1999. Midkine gene expression in the healing process of gastric ulcer. J Lab Clin Med 133:349–352.

Matsumoto K, Wanaka A, Takatsuji K, Muramatsu H, Muramatsu T, Tohyama M. 1994. A novel family of heparin-binding growth factors, pleiotrophin and midkine, is expressed in the developing rat cerebral cortex. Brain Res Dev Brain Res 79:229–241.

Matsuzawa M, Muramatsu T, Yamamori T, Knoll W, Yano R. 1999. Novel neuronal effects of midkine on embryonic cerebellar neurons examined using a defined culture system. Cell Mol Neurobiol 19:209–221.

Michikawa M, Kikuchi S, Muramatsu H, Muramatsu T, Kim SU. 1993. Retinoic acid responsive gene product, midkine, has neurotrophic functions for mouse spinal cord and dorsal root ganglion neurons in culture. J Neurosci Res 35:530–539.

Mitsiadis TA, Salmivirta M, Muramatsu T, Muramatsu H, Rauvala H, Lehtonen E, Jalkanen M, Thesleff I. 1995. Expression of the heparin-binding cytokines, midkine (MK) and HB-GAM (pleiotrophin) is associated with epithelial-mesenchymal interactions during fetal development and organogenesis. Development 121:37–51.

Mochizuki R, Takeda A, Sato N, Kimpara T, Onodera H, Itoyama Y, Muramatsu T. 1998. Induction of midkine expression in reactive astrocytes following rat transient forebrain ischemia. Exp Neurol 149:73–78.

Muramatsu T. 1994. The midkine family of growth/differentiation factors. Dev Growth Differ 36:1–8.

Muramatsu H, Muramatsu T. 1991. Purification of recombinant midkine and examination of its biological activities: functional comparison of new heparin binding factors. Biochem Biophys Res Commun 177:652–658.

Muramatsu H, Shirahama H, Yonezawa S, Maruta H, Muramatsu T. 1993. Midkine, a retinoic acid-inducible growth/differentiation factor: immunochemical evidence for the function and distribution. Dev Biol 159:392–402.

Nakamoto M, Matsubara S, Miyauchi T, Obama H, Ozawa M, Muramatsu T. 1992. A new family of heparin binding growth/differentiation factors: differential expression of the midkine (MK) and HB-GAM genes during mouse development. J Biochem 112:346–349.

Ohta S, Muramatsu H, Senda T, Zou K, Iwata H, Muramatsu T. 1999. Midkine is expressed during repair of bone fracture and promotes chondrogenesis. J Bone Miner Res 14:1132–1144.

Oyanagi K, Kakita A, Kawasaki K, Hayashi S, Yamada M. 2001. Expression of calbindin D-28k and parvalbumin in cerebral cortical dysgenesis induced by administration of ethylnitrosourea to rats at the stage of neurogenesis. Acta Neuropathol 101:375–382.

Oyanagi K, Kakita A, Yamada M, Kawasaki K, Hayashi S, Ikuta F. 1998. Process of repair in the neuroepithelium of developing rat brain during neurogenesis: chronological and quantitative observation of DNA-replicating cells. Brain Res Dev Brain Res 108:229–238.

Oyanagi K, Yoshida Y, Ikuta F. 1986. The chronology of lesion repair in the developing rat brain: biological significance of the preexisting extracellular space. Virchows Arch A Pathol Anat Histopathol 408:347–359.

Oyanagi K, Yoshida Y, Ikuta F. 1987. Selectivity of cell degeneration and histological peculiarities of the repair process in the developing rat spinal cord after ethylnitrosourea administration. Brain Nerve 39:1077–1082.

Oyanagi K, Yoshida Y, Ikuta F. 1988. Cyto-architectonic investigation of the rat spinal cord following ethylnitrosourea administration at different developmental stages. Virchows Arch A Pathol Anat Histopathol 412:215–224.

Qiu L, Escalante CR, Aggarwal AK, Wilson PD, Burrow CR. 2000. Monomeric midkine induces tumor cell proliferation in the absence of cell-surface proteoglycan binding. Biochemistry 39:5977–5987.

Paxinos G, Ashwell KWS, Törk I. 1994. Atlas of the developing rat nervous system, Second ed. San Diego: Academic Press.

Ratovitski EA, Kotzbauer PT, Milbrandt J, Lowenstein CJ, Burrow CR. 1998. Midkine induces tumor cell proliferation and binds to a high affinity signaling receptor associated with JAK tyrosine kinases. J Biol Chem 273:3654–3660.

Satoh J, Muramatsu H, Moretto G, Muramatsu T, Chang HJ, Kim ST, Cho JM, Kim SU. 1993. Midkine that promotes survival of fetal human neurons is produced by fetal human astrocytes in culture. Brain Res Dev Brain Res 75:201–205.

Shimada M, Langman J. 1970. Repair of the external granular layer of the hamster cerebellum after prenatal and postnatal administration of methylazoxymethanol. Teratology 3:119–134.

Sun XZ, Inouye M, Fukui Y, Hisano S, Sawada K, Muramatsu H, Muramatsu T. 1997. An immunohistochemical study of radial glial cells in the mouse brain prenatally exposed to γ-irradiation. J Neuropathol Exp Neurol 56:1339–1348.

Sun XZ, Takahashi S, Fukui Y, Hisano S, Kuboda Y, Sato H, Inouye M. 1999. Different patterns of abnormal neuronal migration in the cerebral cortex of mice prenatally exposed to irradiation. Brain Res Dev Brain Res 114:99–108.

Swann PF, Magee PN. 1971. Nitrosamine-induced carcinogenesis. The alkylation of N-7 of guanine of nucleic acids of the rat by diethylnitrosamine, *N*-ethyl-*N*-nitrosourea and ethyl methanesulphonate. Biochem J 125:841–847.

Wada M, Kamata M, Aizu Y, Morita T, Hu JG, Oyanagi K. 2002. Alteration of midkine expression in the ischemic brain of humans. J Neurol Sci 200:67–73.

Wang SY, Yoshida Y, Goto M, Moritoyo T, Tsutsui J, Izumo S, Sato E, Muramatsu T, Osame M. 1998. Midkine exists in astrocytes in the early stage of cerebral infarction. Brain Res Dev Brain Res 106:205–209.

Yoshida Y, Goto M, Tsutsui J, Ozawa M, Sato E, Osame M, Muramatsu T. 1995. Midkine is present in the early stage of cerebral infarct. Brain Res Dev Brain Res 85:25–30.

Yoshida Y, Oyanagi K, Ikuta F. 1984. Initial cellular damage in the developing rat brain caused by cytotoxicity of ethylnitrosourea. Brain Nerve 36:175–182.

Available online at www.sciencedirect.com
SCIENCE DIRECT
Neuroscience Letters 394 (2006) 5–8
Neuroscience Letters
www.elsevier.com/locate/neulet

Acute limbic encephalitis: A new entity?

Yoko Mochizuki [a,*], Toshio Mizutani [a], Eiji Isozaki [b], Toshiyuki Ohtake [b], Yukitoshi Takahashi [c]

[a] *Department of Pathology, Tokyo Metropolitan Neurological Hospital, 2-6-1 Musashidai, Fuchu-shi, Tokyo 183 0042, Japan*
[b] *Department of Neurology, Tokyo Metropolitan Neurological Hospital, Tokyo 183 0042, Japan*
[c] *Department of Pediatrics, National Epilepsy Center, Shizuoka Institute of Epilepsy and Neurological Disorders, Shizuoka 420 8688, Japan*

Received 3 May 2005; received in revised form 15 August 2005; accepted 22 August 2005

Abstract

Clinical cases similar to herpes simplex virus (HSV) encephalitis have accumulated in Japan. Detailed examinations have failed to demonstrate HSV infection. Recently, these cases have been named "non-herpetic acute limbic encephalitis". Only a single autopsy case was so far reported in an abstract form, because many cases showed a good prognosis. The case presented here was that following fever, a 59-year-old woman developed disturbance of consciousness and uncontrollable generalized seizures. Brain MRI revealed abnormal signals in the bilateral medial temporal lobe and along the lateral part of the putamen. Autoantibody against the NMDA glutamate receptor (GluR) IgM-ε2 was detected in the serum, and the GluR IgG-δ2 antibody was positive in cerebrospinal fluid. She died 12 days after onset. An autopsy examination revealed scattered foci consisting of neuronal loss, neuronophagia and some perivascular lymphocytic infiltration in the hippocampus and amygdala, but no haemorrhagic necrosis in the brain. HSV-1, -2 and human herpes virus-6 were negative immunohistochemically. We believe that our autopsy case may contribute to understanding the neuropathological background of non-herpetic acute limbic encephalitis.

Keywords: Acute encephalitis; Status epilepticus; Autopsy; Non-herpetic acute limbic encephalitis; Herpes simplex encephalitis

Limbic encephalitis is usually considered to be paraneoplastic, occurring subacutely in association with specific neuronal antibodies [2]. Among the cases with reversible acute or subacute non-paraneoplastic limbic encephalitis, voltage-gated potassium channel (VGKC) antibodies have been reported [12]. Autoantibodies against the NMDA glutamate receptor (GluR), which is considered to be related causally to partial seizures [11], were detected in the acute non-herpetic encephalitis [3].

In Japan, acute encephalitis, in which the clinical picture was comparable with that of herpes simplex virus (HSV) encephalitis but where evidence of HSV infection was not demonstrated, has been reported [5]. Recently, these cases have been named "non-herpetic acute limbic encephalitis" as a possible new subgroup of limbic encephalitis [5,9]. It has been proposed that mild infections and immunological process are the cause of this disease from clinical findings and cerebrospinal fluid (CSF) cytokine levels, elevated level of interleukin-6 [5,9] and unelevated level of interferon-γ [1]. Moreover, it has been indicated that acute limbic encephalitis, HSV encephalitis and other acute limbic encephalitis were etiologically interrelated, because cases of limbic encephalitis similar to non-herpetic acute limbic encephalitis were reported [1,9].

Many previously reported cases of non-herpetic acute limbic encephalitis have shown a rather favorable prognosis [1,4,5,7,8,10]. For this reason, only a single autopsy case was so far reported in an abstract form [7]. We believe that this report contributes to understanding the neuropathological background of the acute limbic encephalitis of unknown etiology.

One week after a fever, a 59-year-old woman developed progressive disturbance of consciousness following generalized tonic seizures. The brain computed tomography showed no abnormalities. CSF examinations showed mononuclear cells 10 μl/l, protein 50 mg/dl and glucose 143 mg/dl. The seizures continued, even though multiple anticonvulsants were administered and mechanical ventilation was performed. Eight days after the onset of unconsciousness and seizures, brain magnetic resonance imaging (MRI) with T2-weighted and FLAIR images revealed high signal intensities in the bilateral medial temporal lobes and along the lateral part of the putamen (Fig. 1). She was admitted to our hospital 10 days after the onset of the seizures. She showed marked emaciation and pneumonia complications. Recurrence of generalized tonic seizures

* Corresponding author. Tel.: +81 423 23 5110; fax: +81 423 22 6219.
E-mail address: mochi@ica.nihon-u.ne.jp (Y. Mochizuki).

0304-3940/$ – see front matter © 2005 Elsevier Ireland Ltd. All rights reserved.
doi:10.1016/j.neulet.2005.08.070

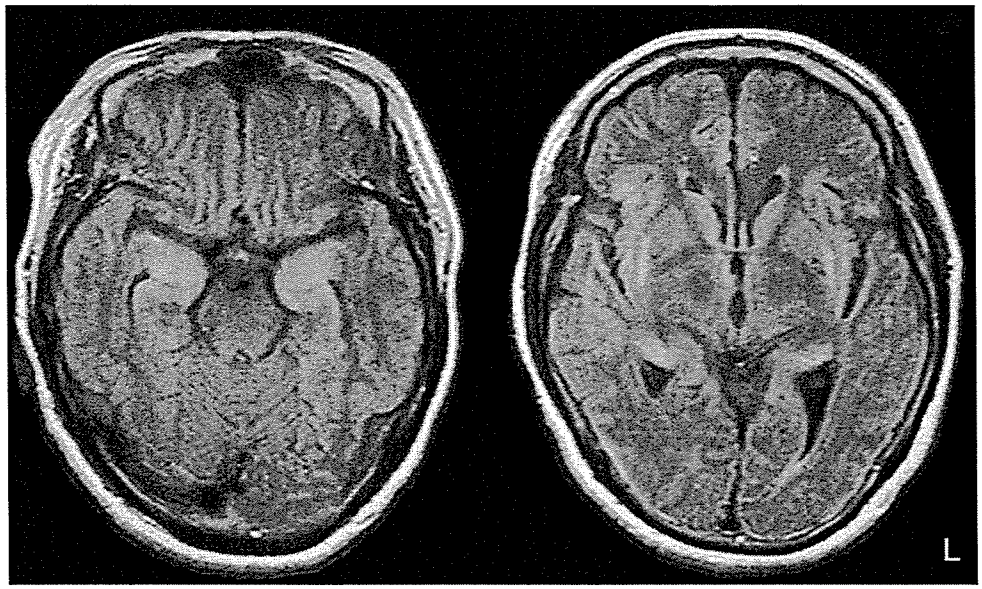

Fig. 1. FLAIR MRI images. High signal intensity is seen in the bilateral medial temporal lobe and the lateral part of the putamen.

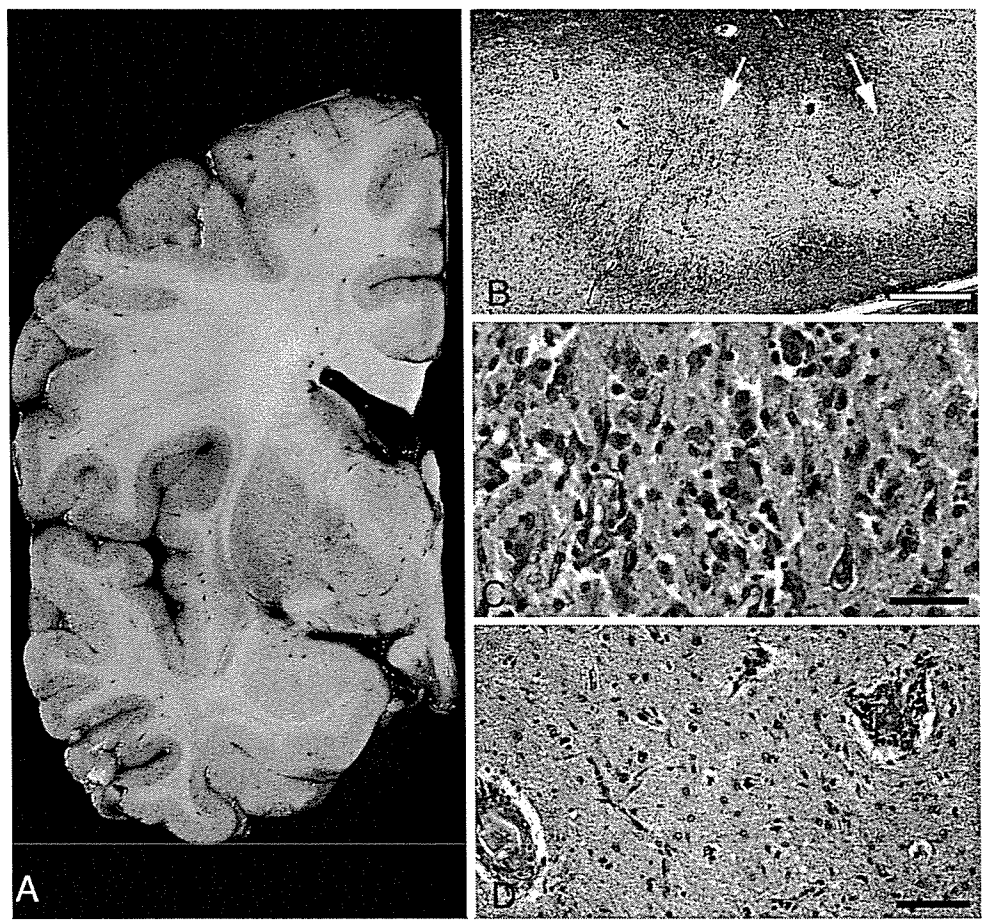

Fig. 2. Neuropathological findings: (A) coronal slice through the left cerebrum. No lesions visible on macroscopic examination; (B) foci of neuronal loss (arrows) surrounded by spongy state in the rostral CA1 of hippocampus. Klüver–Barrera staining (Bar 500 μm); (C) foci of neuronal loss and neuronophagia in the rostral CA1 of hippocampus. Hematoxylin and eosin (HE) staining (Bar 50 μm) and (D) neuronal loss, fibrillary astrocytosis and lymphocytic perivascular cuffing were seen in the rostral part of amygdala. HE staining (bar 50 μm).

failed to be controlled with propofol and acyclovir in addition to the anticonvulsants. An electroencephalogram revealed multifocal spikes without periodic synchronous discharges and periodic lateralized epileptiform discharges. Autoantibodies, including antinuclear antibody, anti-SS-A/B antibodies, and anti-Hu antibodies were all negative. Autoantibody against the GluR IgM-ε2 [11] in the serum was positive, autoantibody against GluR IgG-δ2 in the CSF was positive, and VGKC antibody and P/Q-type voltage-gated calcium channel antibodies were negative in the serum and CSF. Antibodies for several viruses including HSV in the serum and CSF were negative 10 days after the onset of seizures. She had acute renal failure complications and died 12 days after the onset of the seizures.

The direct cause of death was acute renal tubular necrosis and purulent pneumonia. Both laboratory data and pathological examination revealed that the patient did not have any malignant tumors or collagen disease. The brain, weighing 1183 g, was macroscopically unremarkable except for mild swelling (Fig. 2A). Microscopically, there were no leptomeningitis. The amygdala and hippocampus showed small foci of neuronal loss with neuronophagias, proliferation of microglias and hypertrophic astrocytes (Fig. 2B and C). These foci were surrounded by a spongy state. Only a few lymphocytic perivascular cuffings occurred in the amygdala (Fig. 2D). No intranuclear inclusion bodies were found anywhere. Immunohistochemistry for HSV-1, -2 and human herpesvirus-6 was negative. No tissue necrosis or haemorrhage were found in the cerebral cortex including the cingulate, insular, and parahippocampal cortex.

Besides demonstrating evidence of HSV infection, HSV encephalitis shows extensive necrosis with haemorrhage in the medial temporal lobe, insular and cingulate gyri bilaterally [6], where the brain MRI shows high signal intensities. Furthermore, the lesions are bilateral, but not always symmetrical in distribution. In our case, however, abnormal signal intensities were limited in the hippocampus and amygdala bilaterally and symmetrically. No haemorrhagic necrosis was found anywhere, even though there would not have been sufficient time for our patient to develop it. Finally, there were no intranuclear inclusions or immunohistological evidence of HSV infection.

Recently, it is suggested that the presence of autoantibodies against the GluR-ε2 in the CSF of non-herpetic acute encephalitis involves in autoimmune pathogenic mechanism [3,9]. In the CSF of this patient, autoantibody against the GluR-ε2 was negative, while the autoantibody against the GluR-δ2, which is against cerebellar Purkinje cell-specific antibody [11] was positive. The other similar cases as shown in Table 1 [1,4,5,7,8,10] were not examined for the presence of these antibodies. Unfortunately, it remains obscure that this antibody played a role in development of the disease in our case.

There has been only one pathological report of a patient similar to our case: a 53-year-old woman who died 36 days after the onset of illness, and showed neuronal loss in the hippocampus, and neuronophagia and gliosis in the amygdala [7]. As seen in the present patient, this patient showed no evidence of HSV infection, no apparent necrosis in the brain, and the

Table 1
Clinical characteristics and MRI abnormalities of patients with non-herpetic acute limbic encephalitis

Patients	Kohira et al. [4]	Kusuhara et al. [5]				Asaoka et al. [1]					Nonaka et al. [8]	Takahashi et al. [10]		Maki et al. [7]	Present case
		Case 1	Case 2	Case 3	Case 4	Case 1	Case 2	Case 3	Case 4	Case 5	Case 6	Case 1	Case 2		
Age (year)	25	40	38	38	53	34	60	73	35	23	18	42	25	58	53	59
Sex	M	M	F	M	F	M	F	F	M	M	F	F	F	M	F	F
Clinical symptoms																
Impaired consciousness	2+	3+	3+	+	3+	2+	+	2+	2+	2+	2+	3+	+	+	3+	3+
Seizures	2+	2+	3+	+	–	+	+	+	2+	+	3+	3+	2+	–	3+	3+
Cerebrospinal fluid																
Cells (mm^3)	52	17	47	9	10	10	5	32	8	5	320	10	1	76	normal	10
Protein(mg/dl)	25	325	55	27	50	72	32	29	41	28	86	40	15	45	normal	50
MRI abnormalities																
Hippocampi	B	B	B	B	L	B	R>L	B	B	B	L>R	B	B	B	B	B
Amygdalae	B	B	B	B	L	B	R>L	B	B	B	L>R	B	B	B	B	B
Cingulate gyri	–	–	L	–	–	–	–	B	–	–	–	–	–	–	–	–
Sequelae	+	+	+	+	+	+	2+	2+	+	+	+	+	+	+	died	died

M: male; F: female; B: bilateral; L: left; R: right, (−): negative; (+): mild; (2+): moderate and (3+): severe.

lesions were exclusively limited to the hippocampus and amygdala. In this regard, similar clinical cases with acute encephalitis have accumulated in Japan, as shown in Table 1 [1,4,5,7,8,10]. Many cases with this type of encephalitis showed good prognosis, although patients died because of uncontrollable generalized seizures during the clinical course. It is likely that our case showed the neuropathological changes of non-herpetic acute limbic encephalitis as a possible clinicopathological new entity.

Acknowledgements

The authors gratefully acknowledge Dr. Tetsutaro Sata, Department of Pathology, National Institute of Infectious Disease, and Dr. Makoto Shibuya, Department of Pathology, Tokai University Hachioji Hospital for performing immunohistochemistry; Drs. Masakatsu Motomura and Hirokazu Shiraishi, First Department of Internal Medicine Graduate School of Biomedical Sciences Nagasaki University for measurement of the antibodies against voltage-gated potassium channels and P/Q-type voltage-gated calcium channels; Dr. Satoshi Kamei, Division of Neurology, Department of Medicine, Nihon University School of Medicine for valuable comments.

References

[1] K. Asaoka, H. Shoji, S. Nishizaka, M. Ayabe, T. Abe, N. Ohori, T. Ichiyama, Y. Eizuru, Non-herpetic acute limbic encephalitis: cerebrospinal fluid cytokines and magnetic resonance imaging findings, Intern. Med. 43 (2004) 42–48.

[2] J. Dalmau, F. Graus, Paraneoplastic syndromes of the nervous system, in: P.M. Black, J.S. Loeffler (Eds.), Cancer of the Nervous System, Blackwell Scientific, Cambridge, MA, 1997, pp. 674–700.

[3] S. Kamei, Acute juvenile female non-herpetic encephalitis (AJFNHE), Shinkei Kenkyu no Shinpo 48 (2004) 827–836 (in Japanese with English abstract).

[4] I. Kohira, T. Shohmori, S. Kuroda, A. Kanzaki, H. Higashi, Y. Higashi, S. Higashi, A. Handa, K. Kinoshita, K. Terasaka, H. Sugatani, T. Higashi, A case of encephalitis with MRI abnormalities localized in the bilateral amygdala and hippocampus, No to Shinkei 44 (1992) 649–653 (in Japanese with English abstract).

[5] T. Kusuhara, H. Shoji, M. Kaji, M. Ayabe, H. Hino, Non-herpetic acute limbic encephalitis, Rinsho Shinkeigaku 34 (1994) 1083–1088 (in Japanese with English abstract).

[6] S. Love, C.A. Wiley, Viral diseases, in: D.I. Graham, P.L. Lantos (Eds.), Greenfield's Neuropathology, vol. 2, Seventh ed., Edward Arnold, London, 2002, pp. 1–105.

[7] T. Maki, Y. Kokubo, S. Nishida, H. Suzuki, S. Kuzuhara, An autopsy case of non-herpetic limbic encephalitis, Neuropathology 24 (2004) A27 (Abstract ID-15).

[8] M. Nonaka, N. Ariyoshi, T. Shonai, M. Kashiwagi, T. Imai, S. Chiba, H. Matsumoto, CT perfusion abnormalities in a case of non-herpetic acute limbic encephalitis, Rinsho Shinkeigaku 44 (2004) 537–540 (in Japanese with English abstract).

[9] H. Shoji, M. Ayabe, K. Sakai, Non-herpetic acute limbic encephalitis, Shinkei Kenkyu no Shinpo 48 (2004) 821–826 (in Japanese with English abstract).

[10] T. Takahashi, S. Kamei, K. Miki, K. Ogawa, T. Mizutani, The analysis of cytokines in cerebrospinal fluid (CSF) in two cases of non-herpetic acute limbic encephalitis (NHALE), Rhinsho Shinkeigaku 43 (2003) 162–169 (in Japanese with English abstract).

[11] Y. Takahashi, H. Mori, M. Mishina, M. Watanabe, T. Fujiwara, J. Shimomura, H. Aiba, T. Miyajima, Y. Saito, A. Nezu, H. Nishida, K. Imai, N. Sakaguchi, N. Kondo, Autoantibodies to NMDA receptor in patients with chronic forms of epilepsia partialis continua, Neurology 61 (2003) 891–896.

[12] A. Vincent, C. Buckley, J.M. Schott, I. Baker, B.-K. Dewar, N. Detert, L. Clover, A. Parkinson, C.G. Bien, S. Omer, B. Lang, M.N. Rossor, J. Palace, Potassium channel antibody-associated encephalopathy: a potentially immunotherapy-responsive form of limbic encephalitis, Brain 127 (2004) 701–712.

Acta Neuropathol (2005) 110: 255–260
DOI 10.1007/s00401-005-1044-2

REGULAR PAPER

Toshiki Uchihara · Ayako Nakamura · Yoko Mochizuki
Masaharu Hayashi · Satoshi Orimo · Eiji Isozaki
Toshio Mizutani

Silver stainings distinguish Lewy bodies and glial cytoplasmic inclusions: comparison between Gallyas-Braak and Campbell-Switzer methods

Received: 1 May 2005 / Revised: 17 May 2005 / Accepted: 17 May 2005 / Published online: 8 July 2005

Abstract Lewy bodies (LBs) of idiopathic Parkinson's disease and glial cytoplasmic inclusions (GCIs) of multiple system atrophy are pathological deposits both composed of phosphorylated α-synuclein woven into different filaments. Although both LBs and GCIs are considered to be hallmarks for each independent synucleinopathy, until now they could not be clearly distinguished on the basis of their biochemical or immunohistochemical features. We have examined possible differences in their argyrophilic features and their relation to synuclein-like or ubiquitin-like immunoreactivity (IR). Pairs of mirror sections from different brain areas were triple-fluorolabeled with an anti-α-synuclein antibody, an anti-ubiquitin antibody and thiazin red (TR), a fluorochrome that labels fibrillary structures such as Lewy bodies or neurofibrillary tangles. One of the paired sections was subsequently stained using the Campbell-Switzer method (CS), and the other by the Gallyas-Braak method (GB). By comparing of the same microscopic field on the paired fluorolabeled sections, subsequently silver-stained with either CS or GB, five different profiles of each structure could be determined: α-synuclein-like IR, ubiquitin-like IR, affinity to TR, argyrophilia with CS or GB. GCIs exhibited argyrophilia with both CS and GB but lacked affinity to TR. In contrast, LBs exhibited argyrophilia with CS but not with GB and some affinity to TR. These disease-specific profiles of argyrophilia were consistent, and were not influenced by areas or cases examined. Although immunohistochemical features of LBs and GCIs were similar in exhibiting IR for α-synuclein and ubiquitin, the contrast in their argyrophilic profiles may indicate possible differences in the molecular composition or conformation of α-synuclein. Even though these empirical differences still remain to be explained, awareness of this clear distinction is potentially of diagnostic and pathological relevance.

Keywords Argyrophilia · Campbell-Switzer · Diagnosis · Gallyas-Braak · α-Synuclein

T. Uchihara (✉) · A. Nakamura
Department of Neuropathology, Tokyo Metropolitan Institute for Neuroscience, 2-6 Musashi-dai, Fuchu, 183-8526 Tokyo, Japan
E-mail: uchihara@tmin.ac.jp
Tel.: +81-42-3253881 ext 4712
Fax: +81-42-3218678

Y. Mochizuki · T. Mizutani
Department of Pathology,
Tokyo Metropolitan Neurological Hospital,
Tokyo, Japan

M. Hayashi
Department of Clinical Neuropathology,
Tokyo Metropolitan Institute for Neuroscience, Tokyo, Japan

S. Orimo
Department of Neurology, Kanto Central Hospital, Tokyo, Japan

E. Isozaki
Department of Neurology,
Tokyo Metropolitan Neurological Hospital, Tokyo, Japan

Introduction

Lewy bodies (LBs) of Parkinson's disease (PD) and glial cytoplasmic inclusions (GCIs) of multiple system atrophy (MSA) are pathological deposits containing phosphorylated α-synuclein as one of their major constituents [5]. These diseases are grouped under the name "synucleinopathies" based on the assumption that LBs and GCIs share common mechanism for α-synuclein deposition [7]. Indeed, biochemical and immunohistochemical features of these deposits look so alike that a clear distinction between the two types of deposits using these methods is still difficult.

Another method to identify these deposits is silver staining [2, 15]. Our previous studies on argyrophilic features of sporadic degenerative tauopathies demonstrated that silver staining profiles are closely related to tau deposits in a disease- or isoform-specific fashion. Deposits containing mainly three-repeat (3R) tau, such as Pick bodies [23], are labeled by Campbell-Switzer silver staining method (CS) [4, 16]. In contrast, those

containing mainly four-repeat (4R) tau, as seen in corticobasal degeneration (CBD)/progressive supranuclear palsy (PSP) [21] and argyrophilic grains [22], are silver-stained using the Gallyas-Braak method (GB) [3, 6]. Neurofibrillary tangles of Alzheimer type, containing both 3R and 4R tau, are stained with both CS and GB [21, 22, 23]. These findings led us to conclude that 3R tau deposits are related to CS and 4R tau deposits to GB. It means that each method of silver staining exhibits argyrophilia in different ways and potentially represents underlying molecular or "qualitative" differences.

Expecting that similar qualitative differences, distinguishable with silver staining, may be present among α-synuclein-positive deposits, we were prompted to examine their argyrophilic profiles with CS and GB. This is the first study demonstrating disease-specific profiles of argyrophilia in synucleinopathies.

Materials and methods

Six cases of MSA and five cases of PD were enrolled into this study. Demographic data on these cases are shown in Table 1. Clinical diagnosis of PD was based on levodopa-responsive parkinsonism with tremor, rigidity, and bradykinesia, and was confirmed pathologically in all the cases by the presence of LBs and neuronal depletion in the substantia nigra, locus ceruleus and dorsal motor nucleus of vagus. Clinical diagnosis of MSA was differentiated from PD by concomitant ataxia (with cerebellar atrophy demonstrated by brain imaging), marked pyramidal signs and profound autonomic dysfunction. Pathological confirmation of MSA was based on the degeneration in the putamen, substantia nigra, pons, inferior olive and cerebellum and the presence of GCIs [12, 13].

Brains were fixed in formalin and embedded in paraffin. Areas rich in α-synuclein-positive deposits (motor cortex, putamen, pontine nucleus and cerebellum for MSA; limbic cortex, nucleus basalis of Meynert, amygdala, midbrain and medulla oblongata for PD) were examined for their argyrophilia with GB and CS on adjacent sections.

In addition, mirror section pairs (4 μm thick) from these areas were subjected to subsequent studies to identify possible relation between α-synuclein-like immunoreactivity (IR), ubiquitin-like IR and argyrophilia. Pairs of mirror sections were autoclaved and incubated at 4°C for 2 days with a mixture of an anti-synuclein mouse monoclonal antibody (1:200, LB509; a generous gift from Prof. T Iwatsubo, University of Tokyo [11]) and an anti-ubiquitin rabbit polyclonal antibody (DAKO, Glostrup, Denmark) and the target epitopes were visualized with an anti-mouse IgG conjugated with Alexa 488 (1:200; Molecular Probes, Eugene, OR) and an anti-rabbit IgG conjugated with Alexa 647 (1:200; Molecular Probes). Sections were then incubated with thiazin red (TR; 1:30,000; Wako, Tokyo, Japan), a fluorochrome that labels fibrillary structures such as LBs [14] or NFTs [18, 19] for 15 min. After being observed under a confocal microscope (Leica TCS/SP, Heidelberg, Germany), one of the section pair was stained with GB [3, 6] and the other with CS [4, 16] to compare argyrophilic properties of each α-synuclein-, ubiquitin- or TR-positive structure. Identification of the same microscopic field on the fluorescence images (α-synuclein, ubiquitin and TR) and on the corresponding silver-stained (GB and CS) pair-wise images allowed us to compare staining profiles of each structure based on five different properties; α-synuclein IR, ubiquitin IR, affinity to TR, argyrophilia with GB and that with CS [21, 22, 23]

Results

GCIs exhibited argyrophilia with both CS (Fig. 1A, C) and GB (Fig. 1B, D) to an equivalent extent. Argyrophilia of LBs were clearly detectable with CS (Fig. 1E, G). However, LBs identified on GB-stained sections (Fig. 1F, H) were, at most, weakly argyrophilic (arrow in Fig. 1F, H). These argyrophilic features were consistent and were not influenced by the case or area examined.

Relation of these argyrophilic structures to α-synuclein-like IR and ubiquitin-like IR was examined on paired sections that were initially fluorolabeled and then silver stained (Fig. 2). On the triple-fluorolabeled sections from MSA patients (Fig. 2a–d), most GCIs exhibited α-synuclein-like IR (green) and ubiquitin-like

Table 1 Demographic data of the cases (*MSA* multiple system atrophy, *PD* Parkinson's disease)

Pathological diagnosis	Clinical diagnosis	Age at death (years)	Duration (years)	Gender	Brain weight (g)
MSA	MSA	47	11	M	1460
MSA	MSA	57	6	F	1138
MSA	MSA	58	7	M	1318
MSA	MSA	60	14	M	1239
MSA	MSA	64	20	M	1059
MSA	MSA	74	4	M	1285
PD	PD	60	20	F	1146
PD	PD	65	4	M	1067
PD	PD	73	4	F	1335
PD	PD	74	2	M	1320
PD	PD	78	4	M	1320

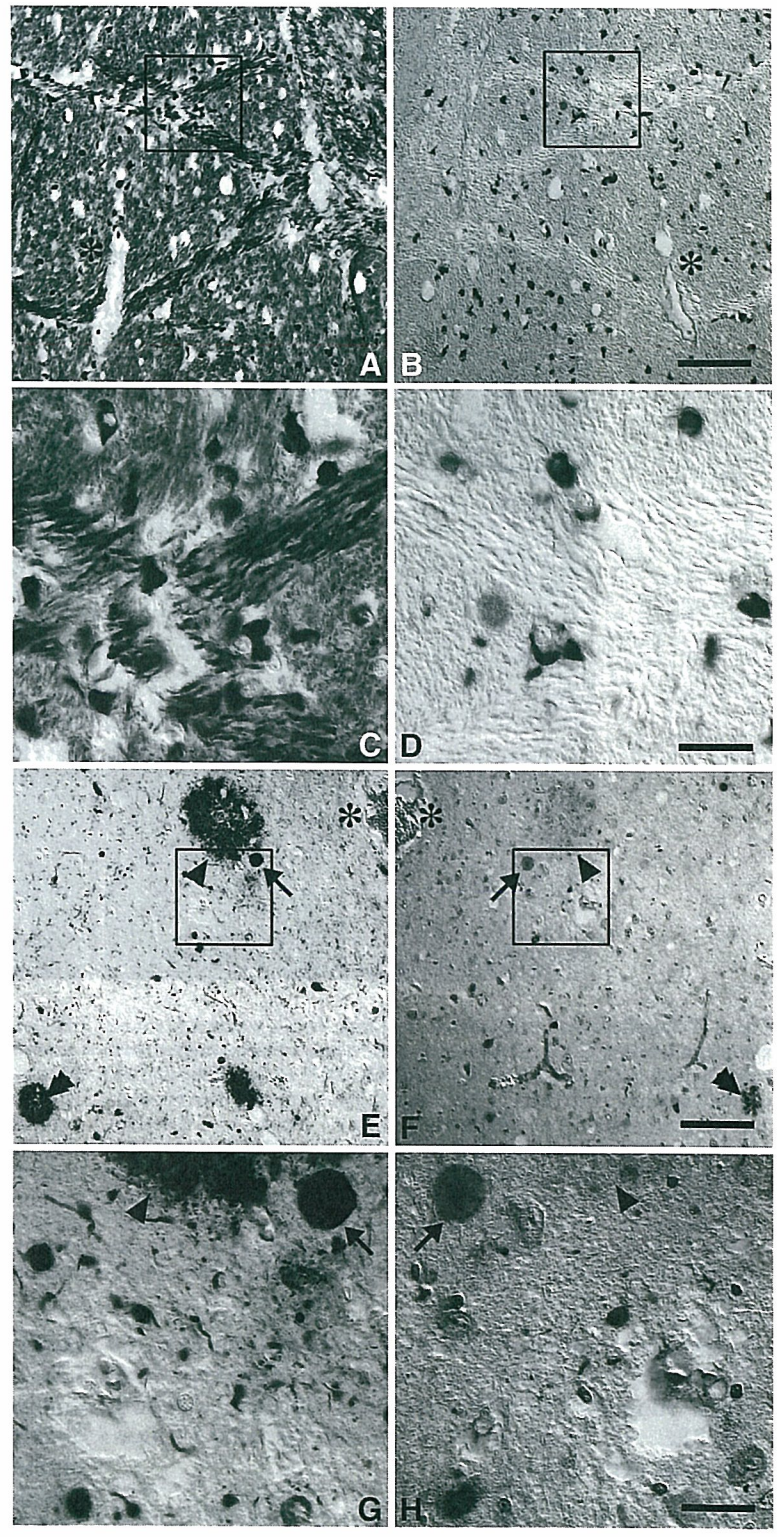

Fig. 1 Silver-stained mirror sections (*left column*: with CS; *right column*: with GB) of MSA (**A–D**) and of PD (**E**, **F**). GCIs in the internal capsule are stained with CS (**A**, **C**). Those in the mirror section pair are similarly stained with GB (**B**, **D**). **C**, **D** Higher magnification of the corresponding *squared area* in **A** and **B**, respectively. LBs in the amygdala are stained with CS (*arrow* in **E**, **G**) but hardly stained with GB (*arrow* in **F**, **H**). Neuritic plaque is stained with CS (*double arrowhead* in **E**) and with GB (*double arrowhead* in **F**), while the diffuse plaque, stained with CS (*arrowhead* in **E**, **G**), is not with GB (*arrowhead* in **F**, **H**). *Asterisk* in **A**, **B** and that in **E**, **F** indicate the same blood vessels in paired mirror sections (*CS* Campbell-Switzer method, *GB* Gallyas-Braak method, *MSA* multiple system atrophy, *PD* Parkinson's disease, *GCIs* glial cytoplasmic inclusions, *LBs* Lewy bodies). *Bars* **A**, **B**, **E**, **F** 100 μm; **C**, **D**, **G**, **H** 25 μm

IR (blue) to yield blue-green color. No affinity to TR (red) was detectable even when the detection threshold was lowered enough to give background myelin staining. Therefore, none of the GCIs appeared white with triple fluorolabeling. Subsequent silver staining of these section pairs demonstrated that GCIs exhibited argyrophilia with both CS (Fig. 2A, C) and GB (Fig. 2B, D) to a similar extent.

On the triple fluorolabeling of mirror section pairs from PD (Fig. 2e–h), most LBs exhibited synuclein-like IR (green) and ubiquitin-like IR (blue) to yield blue-green color. Some of these LBs appeared white as they

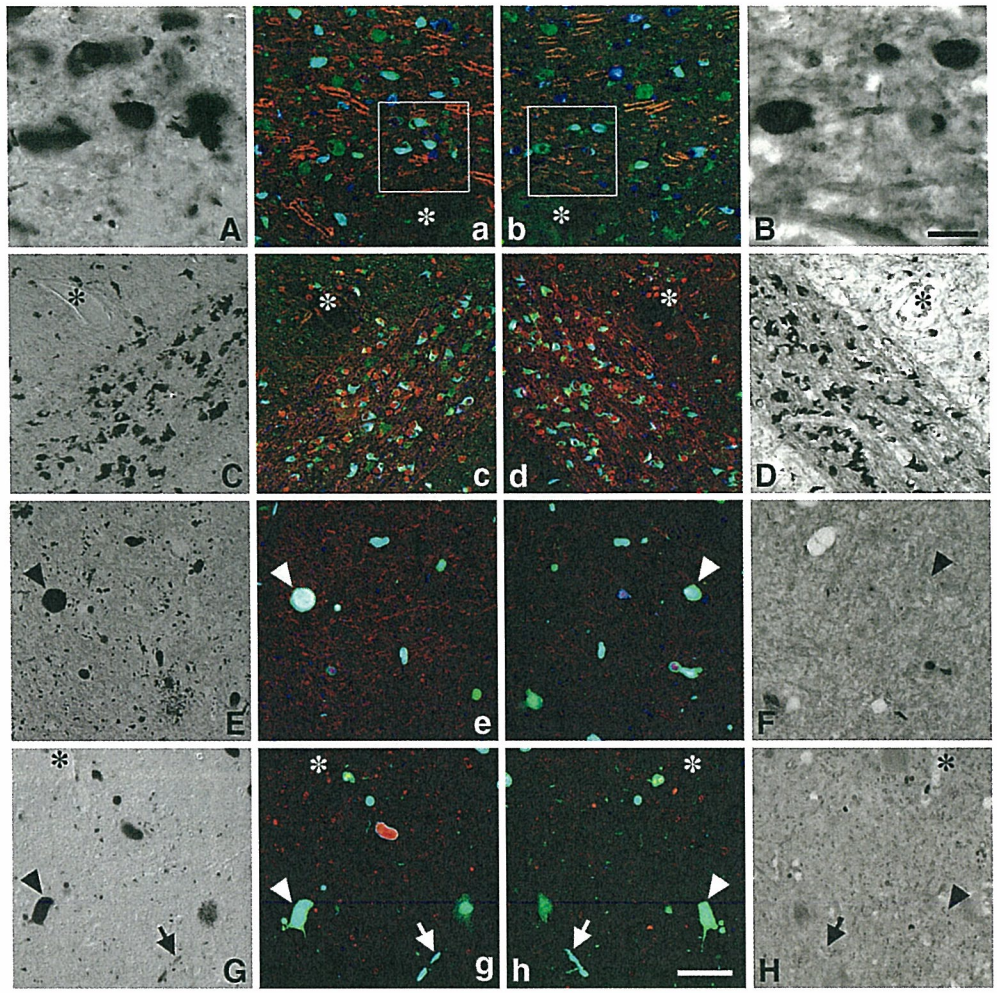

Fig. 2 Triple-fluorolabeled mirror sections (a–g) stained for α-synuclein (*green*), TR (*red*) and ubiquitin (*blue*), subsequently silver stained with CS (**A**, **C**, **E**, **G**) or GB (**B**, **D**, **F**, **H**). GCIs in the cerebellar white matter (**A**, **a**, **b**, **B**) exhibit α-synuclein-like (*green*) and ubiquitin-like (*blue*) IRs, but the lack of affinity to TR (*red*), yielding a blue-green appearance in GCIs. These GCIs are silver stained with CS (**A**, higher magnification of the *squared area* in **a**) and GB (**B**, higher magnification of the *squared area* in **b**). GCIs in the putamen (**C**, **c**, **d**, **D**) exhibited similar IR and silver-staining profiles. LBs in the nucleus basalis of Meynert (**E**, **e**, **f**, **F**), are spherical and exhibit α-synuclein-like (*green*) and ubiquitin-like (*blue*) IRs and affinity to TR (*red*) to yield a whitish appearance (*arrowhead* in **e**, **f**). These LBs are stained with CS (*arrowhead* in **E**) but not with GB (*arrowhead* in **F**). LBs in the dorsal motor nucleus of vagus (*arrowhead* in **G**, **g**. **h**, **H**) are diverse in their morphology but their fluorescence signals (**g**, **h**) are similar to those from LBs in the nucleus basalis (**e**, **f**). Lewy neurites (*arrow* in **G**, **g**, **h**, **H**) share these staining profiles. These LBs (*arrowhead*), as well as Lewy neurites (*arrow*) are stained with CS (**G**) but not with GB (**H**). *Asterisk* in **a**, **b**, **C**, **c**, **d**, **D**, **G**, **g**, **h**, and **H** denotes the same blood vessel observed in paired mirror sections (*TR* thiazin red, *IR* immunoreactivity). *Bars* A, B 10 μm; otherwise 50 μm

also exhibited affinity to TR (red, arrowhead in Fig. 2e, f). All of these LBs, including Lewy neurites, were clearly stained with CS, regardless of their location (Fig. 2E, G). However, GB hardly visualized these structures (Fig. 2F, H).

Discussion

LBs and GCIs are composed of similarly phosphorylated synuclein [5] woven into fibrils and diseases demonstrating these deposits are grouped under the title "synucleinopathies" [7] on the supposition that a common mechanism is involved in the formation of LBs and GCIs. Most of the biochemical and immunohistochemical features related to α-synuclein are shared between LBs and GCIs, and this is one of the reasons why immunohistochemical markers are not very successful in distinguishing the two different synuclein deposits. In the present study, we demonstrated that, using GB and CS, the argyrophilic properties of LBs and GCIs were distinct; i.e., GCIs exhibited argyrophilia with both CS and GB, whereas LBs were labeled by CS but not by GB. These disease-dependent argyrophilic features were consistent, and were not influenced by the case or area examined. We have previously reported that some LBs have an affinity to TR [14], a fluorochrome that labels fibrillary structures, such as NFTs [18, 17, 19]. Comparison of LBs and GCIs clarified that GCIs lacked affinity to TR. Since the differences in molecular com-